ITS/LWR/BNL 85-1
September 1985

Validity of the Use of a Temperature Cutoff for Zircaloy Oxidation:

Experimental Bases

and

Analytical Models

H. Komoriya
P. B. Abramson

INTERNATIONAL TECHNICAL SERVICES INC.
60 East 42nd Street
New York, NY 10165

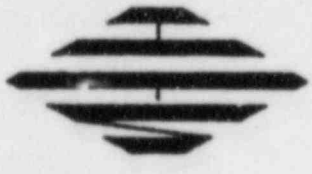

Prepared for:
Brookhaven National Laboratory
Upton, Long Island, New York 18739

Abstract

Available isothermal and non-isothermal experimental data on the reactions of zircaloy with steam at a wide range of temperatures have been reviewed. In particular, results from high temperature experiments at ANL, INEL, PNL, and KFK have been examined to identify and quantify the temperature of and mechanism for oxidation cutoff, therefore hydrogen generation cutoff, during degraded core conditions resulting from severe accidents. Various proposed theoretical mechanisms for oxidation rate limitation were compared with the experimental results, and validity of analyses utilizing computer codes featuring existing models for hydrogen generation and limitation were also assessed.

Summary

Because the reaction of zircaloy with steam is extremely exothermic, if the emergency core coolant system injection is unavailable, an accident such as that experienced at Three Mile Island Unit 2 has a high potential for core melt. Hydrogen generated by such a reaction can accumulate in the containment building, and could, under certain conditions, present additional challenges to containment integrity via its combustion or deflagration in the containment air.

Since the accident at TMI-2, there have been a number of experiments to gain understanding of phenomenology of zircaloy oxidation, including peak temperature, heatup rate, onset of cladding or fuel liquefication and its runoff, channel blockage, etc. In addition, the processes of zircaloy oxidation retardation have also been addressed by the experimenters.

In this report, the available isothermal and non-isothermal experimental data on the reactions of zircaloy with steam at a wide range of temperatures have been reviewed. In particular, results from high temperature experiments at ANL, INEL, PNL, and KfK have been examined to quantify the temperature for oxidation cutoff, therefore hydrogen generation cutoff, during degraded core conditions resulting from severe accidents, and to attempt to identify the mechanisms which cause such cutoff.

The out-of-pile experiment performed at KfK (Hagen experiments) in bundle geometry indicated that the common use by analysts of an absolute oxidation cutoff temperature (of 2400 K) may be physically incorrect. In the ESBU-1 test, the peak temperature reached almost 2500 K, and in addition, there was evidence that liquified zircaloy, which had combined with UO2 to form a eutectic, continued to oxidize after the formation of such a eutectic. A posttest examination revealed that the coolant channels were substantially blocked by molten material.

Preliminary results from PBF Severe Fuel Damage (SFD) Test 1-4 showed that the peak fuel rod temperature rose from 1600 to above 2400 K in less than 3 minutes (posttest calculation using the SCDAP code indicate that temperatures in the range of 2700 K may have been reached, and it is believed that the test may have experienced higher temeperatures for longer times that any previous test) and that a much larger quantity of hydrogen (185 g) was produced than that in either the SFD 1-1 or SFD 1-3 tests (71 and 55 g, respectively). The higher hydrogen production presently is attributed by the experimenters to entrainment of water vapor by the argon sweep gas flowing through the water reservoir. In addition, undetermined quantities of the water vapor were generated by hot bundle material entering the lower plenum water reservoir. Posttest flow measurements indicate that the original flow area through the bundle is about 98 % blocked.

Various theoretical mechanisms have been proposed as presenting potentials for oxidation rate limitation. In this report, these have been compared with the experimental results, and the validity of analyses utilizing computer codes (MARCH, IDCOR's BWR Core Heatup, and SCDAP) featuring existing models for hydrogen generation and limitation are also assessed.

Both the BWR Core Heatup and SCDAP codes appear to handle the computation of the metal-water reaction in a state-of-the-art fashion. Use of the MARCH BWR option enables the user to select any one of the more common parabolic rate constants. However, once selected, the correlation is applied to the entire range of temperature. Selection of Cathcart-Pawel constants is non-conservative since these constants would then be used outside of their valid temperature range which results in under-prediction of the oxidation rate and the associated hydrogen production rate. In addition, because of the lumping of fuel and cladding materials in MARCH, separate melting of the zircaloy is not directly computed. Therefore, under certain accident scenarios, the cladding temperature would be underpredicted which leads to a delayed onset of oxidation and under-estimation of hydrogen generation. In sum, this can lead to a larger uncertainty in the computed results.

Simple modifications to MARCH are recommended to ensure that the user can not select an option which does not give a best-estimate or conservative result. (Baker-Just equation is not conservative in the low temperature range.) To accomplish this, the code should be modified so that the optional selection of Zr oxidation models is no longer limited to just one or the other correlation. Such modification should permit the use of the three different correlations in various combinations over their appropriate temperature ranges.

In addition, it was concluded that there was no physical foundation for the current use of a fixed temperature cutoff for zircaloy oxidation in the severe accident codes such as MARCH, SCDAP and BWR CORE-HEATUP. Nevertheless, experimental evidence does support the view that generation of hydrogen via zircaloy oxidation is retarded by presence of one or more of the following situations: (a) steam starvation, (b) consumption of the zircaloy, and (c) geometry changes which cause changes in the zircaloy surface to volume ratio and in the steam flow access to the area of interest, such as happens during so called candling of liquified fuel and zircaloy. Items (a) and (b) have been modeled in these codes. In place of item (c), these codes make use of the temperature cutoff (SCDAP, however, apparently does have a complex relocation model, but runs so slowly that it is often not used). It is strongly recommended that a simple and fast running model be developed to simulate (i) the geometry changes associated with Zr melt, and (ii) several subsequent relocation modes. This model should then be incorporated into the MARCH code in place of continued use of an artificial and arbitrary temperature cutoff. A conceptual discussion of the ingredients of such models is included in the relevant section.

TABLE OF CONTENTS

LIST OF FIGURES

LIST OF TABLES

1.0 INTRODUCTION.

Detailed studies of the accident at Three Mile Island universally indicated that oxidation of zircaloy and other materials contained in the core did not proceed unchecked. Nevertheless, although the temperatures predicted without consideration of oxidation limiting mechanisms were well beyond the indications of the various measurements in the plant, recently obtained data clearly indicate extensive melting and core slumping. As analytical and experimental studies progressed, it became clear that there were physical and/or chemical mechanisms which limited the oxidation and therefore limited hydrogen generation. Although significant further experimental work on hydrogen generation limiting mechanisms has been performed, no comprehensive analysis of those experiments exists. Furthermore, analysis of the consequences of various accident scenarios is highly sensitive to the assumptions made regarding hydrogen generation limitation. The focus of these uncertainties has been upon the probability of a hydrogen deflagration or detonation in a BWR containment, and remains an issue for a number of BWR plants.

In an effort to identify the temperature dependence of the oxidation rate, there have been a large number of isothermal studies of the zirconium and zircaloy-steam reaction. Agreement among the recent studies has been good in the range from 1000 to 1580 C. Above 1580 C, however, there is considerable scatter in the data due to the difficulty in producing truly isothermal conditions at these high temperatures because of the strong self-heating tendency.

Non-isothermal experiments at the Power Burst Facility (PBF) experiments at INEL and the Hagen experiments at KfK in Germany have provided some degree of understanding of how actual fuel pin structures respond to severe accident sequences followed by quenching. However, because of experimental limitations, the data from those experiments is obtained primarily from post-test examination and therefore gives very

little insight into the transient mechanics.

The purpose of this report is threefold: (1) to present a reasonably complete survey of the state-of-the-art understanding of the mechanisms believed to retard zircaloy oxidation, (2) to review a wide range of experiments to identify support for the current use of a cutoff temperature of zircaloy oxidation, and (3) to assess the validity of analyses utilizing computer codes featuring existing models for hydrogen generation and rate limitation.

Several theoretical mechanisms which have been proposed to limit zircaloy oxidation are briefly summarized in Section 2 of this report, followed by a discussion of the details of the experimental data and models and a comparison with the various theoretical mechanisms in Section 3. In Section 4, the models in the computer codes often used to compute hydrogen generation rates are analyzed. The comments, conclusions and recommendations are presented in Section 5.

2.0 THEORETICAL MECHAMISMS OF ZIRCALOY OXIDATION AND OXIDATION RETARDATION.

During accidents in LWR's which uncover the core, zircaloy exposed to steam at high temperatures reacts to form ZrO_2, even in presence of a large initial excess of hydrogen. The reaction producing zirconium dioxide is an exothermic oxidation reaction with the steam, releasing hydrogen. The combination of the fact that the process is highly exothermic and the fact that the oxidation rate increases with temperature, creates an autocatalytic situation whereby the oxidation rate can increase exponentially.

2.1 Thermodynamics of the Reaction.

The complete reaction with steam is as follows:

$$Zr + 2\ H_2O \rightarrow ZrO_2 + 2H_2$$

The heat of reaction is 6300 J/g Zr just below the melting point and 6530 J/g Zr just above the melting point. Zircaloy melts at 2125 K (1852 C) and the heat of fusion is 230 J/g. The large negative Gibbs free energy for the reaction indicate that complete reaction would be expected even in the presence of a large excess of hydrogen in the steam [1]. The quantity of ZrO_2 formed and the quantity of zirconium reacted are not equivalent (unless the reaction goes to completion) because of the fact that an important portion of the oxygen is dissolved within the metal phase ahead of the outer oxide film.

It has been widely accepted that the mechanism that governs the oxidation of zircaloy is the diffusion of oxygen anions through the anion-deficient ZrO_2 lattice, or through the Zr lattice, or both. A parabolic rate law is usually considered to apply when the reaction rate is controlled by solid-state diffusion. In this formulation, the reaction

rate at high temperatures is described by an expression of the form

$$dW/dt = 1/W \cdot K/2, \text{ or } W^2 = Kt$$

where

W = measure of the extent of the reaction, weight of metal reacted,
t = reaction time,
K = A exp (-B/RT), parabolic reaction rate constant,
A, B = constants,
T = absolute temperature of cladding,
R = gas constant.

The reaction rate thus increases exponentially with temperature and decreases with the reciprocal of the oxide layer thickness. The derivation of this parabolic rate law applies correctly to planer geometry; however, it does not apply precisely for cylindrical or spherical geometry. In addition, this formulation ignores the fact that, in spherical geometry (for which the many of the data were obtained), solid-state diffusion rates are altered by the changing area normal to diffusion as the thickness of the oxide layer becomes an appreciable fraction of the sphere radius.

Often missing from the literature on this subject are the principal assumptions which permit the application of such a simplified rate law. Those assumptions are:

1. the simple parabolic rate law is adequate in describing the process in any geometry (planar, cylindrical, spherical) (which is potentially incorrect, since the parabolic law is an explicit result of performing the derivation in planar geometry);
2. no geometry change throughout reaction;
3. constant specific heat and density of the specimen;
4. approximate formulation of the temperature drop across the oxide film.

As shown in Appendix A, the first assumption is not quite valid. Furthermore, the experiments used to derive the various correlations were not performed in planar geometry and no attempt has been made to reduce the data based upon the geometry actually used. In addition, as the reaction becomes more autocatalytic, the degree of error and uncertainties introduced by this assumption increases; error resulting from not using the geometrically correct form of equation, and uncertainties resulting from the geometry change which enevitablly takes place during melting and relocation.

Similarly, the second assumption that there is no geometry change is incorrect, especially above the zircaloy melting temperature. This is exacerbated by the facts that the details of geometry changes during a severe accident depends on many factors few of which are well understood or easy to model. The third and fourth assumptions require more experimental work in zircaloy oxidation kinetics to assess their appropriateness, but are of lesser impact.

In the low temperature range where the rate of oxidation is much slower, these assumptions are adequate and the data and correlations derived from them show good agreement. However, in the high temperature range where the applicability of these assumptions is questionable, the data and various correlations have a considerable scatter. Because of the large scatter in the experimental data, the experiments have appeared to support the use of a parabolic rate theory for the oxidation process, and the errors introduced by the simplifying assumptions were no greater than the experimental uncertainties. In other words, the uncertainties which exist in performing and controlling these high temperature and highly autocatalytic experiments are so great that the uncertainties introduced by the empirical correlations and models are considered to be inconsequential.

The extent of the reaction, W, is typically determined by measuring

1. the weight reacted per unit area, using gravimetric methods,
2. the thickness of the oxide and stabilized alpha layers from

metallographic cross sections, and

3. the volume of hydrogen evolved per unit area.

2.2 Oxidation Limiting Mechanisms.

Several known theoretical mechanisms which may limit such an autocatalytic process are: (a) steam starvation, (b) consumption of the zircaloy, (c) geometry changes which cause changes in the zircaloy surface to volume ratio and in the steam flow access to the area of interest, such as happens during so called candling of liquefied fuel and zircaloy, (d) hydrogen blanketing. Of these, processes (a), (b), and (c) are well enough understood that presence of any one or all can be either quantified or predicted during an experiment.

2.2.1 Steam Starvation.

Steam starvation refers to a local and instantaneous condition in which the absolute amount of steam available per unit area of specimen surface is not sufficient to sustain the particular parabolic oxidation rate which would have been obtained under steam-saturated conditions. This is a result of the local region oxidizing so rapidly that it simply runs out of oxygen in the available steam, either due to lack of source steam flowrate or due to blockage of steam flow paths.

2.2.2 Consumption of Zircaloy.

When there is a decreasing amount of zircaloy available for reaction, regardless of how much steam is available, the rate of zircaloy oxidation decreases. This is evident from the formulation of the parabolic law which expresses oxidation rate in the reciprocal relationship with the oxide layer thickness (and with O_2 consumption per unit area). The governing phenomenon is the necessity for oxygen to diffuse through the already oxidized layer of zircaloy to reach the unoxidized material.

2.2.3 Geometry Changes.

During the melting and slumping of the molten zircaloy, its surface area to volume ratio decreases markedly. This decreases the local oxidation rate by simply reducing the local surface area. Furthermore, the zircaloy can run down to cooler regions, eventually even refreezing if the temperature is low enough. This process clearly reduces further oxidation of the balance of the zircaloy.

In addition to simple melting and run-off, a solid oxide layer can also be breached through chemical reaction, i.e., dissolution of ZrO_2 into the liquified Zr-O or Zr-U-O phase. None of these processes has been, however, experimentally verified during transient conditions.

Geometry changes accompanying clad ballooning have two direct effects: (i) they separate the zircaloy from the fuel thereby decreasing heat loss from the zircaloy and causing more rapid heat up of the zircaloy itself, and (ii) they may reduce the steam flow channel area thereby reducing steam flow to higher axial regions.

2.2.4 Hydrogen Blanketing.

A large amount of hydrogen produced by oxidation of the zircaloy cladding during the rapid oxidation phase of a transient can effectively blanket the fuel cladding both inside the lattice and outside at the surface, restricting access of steam to the surface and to the unoxidized layer, thereby serving to starve the process. Although the average amount of steam available at that axial position to reach fuel-rod cladding may be large enough (i.e., larger than the "steam-starvation" level), the hydrogen fraction at the local ZrO_2-coolant boundary can remain high because of local hydrodynamic laminar flow conditions. Measured oxidation rate in hydrogen-steam mixture environments with high hydrogen fractions has been shown at low steam pressures to be significantly less than the measured oxidation in pure steam [3]. Experiments focused upon measurement of the

effect of hydrogen have all been performed by introduction of hydrogen into the steam inflow to the experimental channel. Although such experiments may introduce hydrogen uniformly throughout the experiment, they do not replicate the hydrogen concentration gradients expected during the rapid oxidation phase. Thus data on this mechanism are inconclusive. Furthermore, no experimentalist has measured the effect of high hydrogen concentration within the ZrO_2 itself upon the ZrO_2 lattice diffusion constants. Such an experiment could be performed at low temperature and would determine the constants used in the parabolic rate equation.

3.0 EXPERIMENTAL RESULTS.

Studies of the initial stages of isothermal oxidation at high temperatures have presented special problems for experimenters who wished to achieve a high degree of accuracy and self-consistency for kinetics measurements. Accurate temperature measurements are important, especially in systems where there is opportunity for extensive heat transfer between the specimen and its surroundings. In addition it is generally impossible to perform such an oxidation experiment under completely isothermal conditions, a fact that necessitates careful interpretation of the kinetic quantities.

The empirically based parabolic rate constant law governing the water-metal reaction is supported by numerous experiments. However, in most of these instances, the purpose of the experiments was to fine-tune the rate constants within a certain low temperature range, approximately 900-1500 C. Because of the inherent difficulty in holding the temperature constant in a high temperature range during highly exothermic experiments, only a few of these supporting experiments were performed at high temperatures (Zr melting temperature range) and even fewer experiments address the issue of oxidation limiting effects.

3.1 Experiments and Models for Oxidation Rate.

Because of the high conservatism with respect to hydrogen production (often critisized as excessively conservative) in the Baker-Just equation developed in early 1960's to describe the kinetics of the oxidation rate, there have been a large number of isothermal experimental studies carried out to refine the Baker-Just model in the temperature range from about 1100 to 1580 C. This range was of key interest in analysis of large-break loss-of-coolant accidents to demonstrate that emergency core cooling system performance was within the design basis; i.e., in conformance to the requirements of 10 CFR 50 Appendix K. These studies resulted in formulation of empirically based analytical models which compute oxide

Table 3.1. Zircaloy - Steam Oxidation Kinetics

	Principal Investigators	Org.	Heating Technique	Kp A	Kp B Activation Energy	Valid Range in C°	Ref
1.	Baker-Just	ANL	Internal	33.3 x 10+6	-45500	Unspecified	1
2.	Cathcart-Pawel	ORNL	External	2.94 x 10+6	-39940	1050 - 1504	6
3.	Leistikow	KfK	External	5.86 x 10+6	-42400		17
4.	Suzuki	JAERI	External	7.60 x 10+6	-40710	1184 - 1330	20
5.	Biederman	WPI*	Internal	3.10 x 10+5	-33370	982 - 1482	11
				2.32 x 10+3	-27340	649 - 816	
6.	Urbanic-Heidrick	AECL	Internal	2.96 x 10+5	-33420	1000 - 1580	9
				8.79 x 10+5	-33000	1580 - 1850	
7.	Westerman	PNL	Internal	5.22 x 10+5	-34700		19
8.	Aly	KfK	External	9.0 x 10+5	-37800	<1550	16
				3.33 x 10+9	-51100	>1550	
9.	Ocken	EPRI	Internal	3.33 x 10+5	-33590	980 - 1550	14
			External	4.14 x 10+6	-41185	980 - 1550	
			All	1.33 x 10+6	-37790	980 - 1550	

Kp = Reaction rate constant, $W^2 = Kp \cdot t$

A = (mg Zr reacted/cm^2) ^{2}/sec

B = (cal/mole)

*Worcester Politechnic Institute

layer growth rates by an equation expressed in Arrhenius form as a function of cladding temperature and certain properties of the oxide layer thickness built up to that time. The models differ only in the value of the specific constants.

Commonly known and used correlations are summarized in Table 3.1. The four most commonly used models are: a) Baker-Just, b) Cathart, c) Urbanic-Heidrick, and d) Biederman. A brief discussion on each one of these models together with certain others is given in the following section.

3.1.1 Baker-Just.

Condenser discharge experiments were performed using 30- and 60-mil zirconium wires immersed in water from room temperature to 315 C (1500 psi vapor pressure). The wire was melted by the pulse of current, and spherical zirconium droplets were subsequently oxidized, as shown in Fig. 3.1. The reaction was studied with initial metal temperatures, due to the current from the condenser discharge, ranging from 1100 to 4000 C. Because of the hypothesis that the oxidation mechanics was governed by diffusion of oxygen through the oxide layer which formed during the ongoing oxidation process, the resulting data were interpreted in terms of a parabolic rate law which were best fit with a rate constant of 695 (mg Zr/sq cm)^2/s at the melting temperature of 1862 C. The Baker-Just rate equation was obtained as a fit to their own high temperature data combined with the lower temperature data of others [1,2]. The Baker-Just equation is Eq. 1 in Table 3.1.

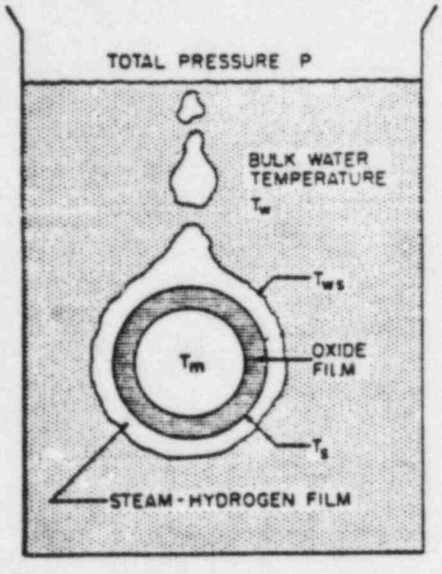

Fig. 3.1. Hot Metal Sphere Reacting with Liquid Water [2]

Following his original experiments, Baker compared his equation with the results of a series of isothermal experiments conducted by Mason and Martin [4] using a "pressure-pulse" method which led to strongly different results and which were the first experimental indication of other rate limiting mechanisms. In this method zirconium was melted in thoria crubiles in a vacuum environment and water vapor at 20 Torr was admitted suddenly by a rapid acting valve. After a fixed reaction period, the residual water vapor and the hydrogen generated were suddenly removed by rapid expansion through another valve to a large volume. The extent of the reaction was determined by analysis of the quantity of hydrogen generated. When the results were compared with values calculated from the fit to his earlier experiments, the measured reaction was an order of magnitude below the predictions. This was attributed by Dr. Baker to a gaseous diffusion limitation of the reaction at such low pressures or a direct effect of the pressure on the reaction rate [1]. Nevertheless, the equation commonly known as the Baker-Just equation is the fit described in the previous paragraph.

3.1.2 Cathcart - Pawel.

A comprehensive study of the oxidation kinetics was carried out mostly with reactor grade zircaloy-4 PWR tubing by Cathcart and his associates at Oak Ridge National Laboratory (ORNL) [5-7]. Two kinds of apparatus were used; the first one, a high thermal inertia furnace system, employed steam preheating as the principal method of temperature control and the temperature of the specimen was not cotrolled directly but was governed by its response to the heat transfer from its steam and furnace environment; the second one, a low thermal inertia furnace system, used a powerful radiant heating furnace where the specimens were subjected to flowing steam during short, precisely documented, temperature excursions. In this case the specimen was controlled directly by regulating the power to the furnace. Both apparatuses utilized the multi-specimen technique to examine reaction kinetics. Complete data were obtained over the temprature range of 900 to 1500 C for the growth of individual layers as well as for the total oxidation. Although the results were close to those of Biederman

(discussed in Section 3.1.4), they were slightly higher near the 1500 C upper limit of the experiments temperature.

The equation predicts a reaction 35 % less than the Baker-Just equation at 1500 C, see Table 3.2 and Fig. 3.2. The authors pointed out that the ratio of the oxide layer thickness to the alpha-layer thickness decreased as temperature increased. This resulted from the higher activation energy for diffusion in the ZrO_2 phase and cannot be extrapolated beyond the temperature of stability of that phase. Oxide layer growth at 900 and 950 C is not well fit by a parabolic curve. Therefore, extrapolation below 1000 C of high temperature rate constant data for oxide layer growth or total oxygen consumption will yield overprediction of these quantities.

The Cathcart group also studied the effect of pressure (500, 100, and 1500 psi), steam flow rate (1 m/s to 18 m/s), and steam injection temperature (150 to 1000 C) on the oxidation kinetics. There were no measurable effects of any of these factors. At 900 C, however, in the region of stability of monoclinic ZrO2, there was a considerable scattering of oxide thicknesses and a variation in oxide structures.

Additions of 10 mole % nitrogen, 10 mole % oxygen or 5 mole % hydrogen to the steam with specimen temperatures of 1101 and 1304 C were shown to have minor, if any, effects on the oxidation rate of zircaloy tubing. Addition of hydrogen consistently resulted in lower rates

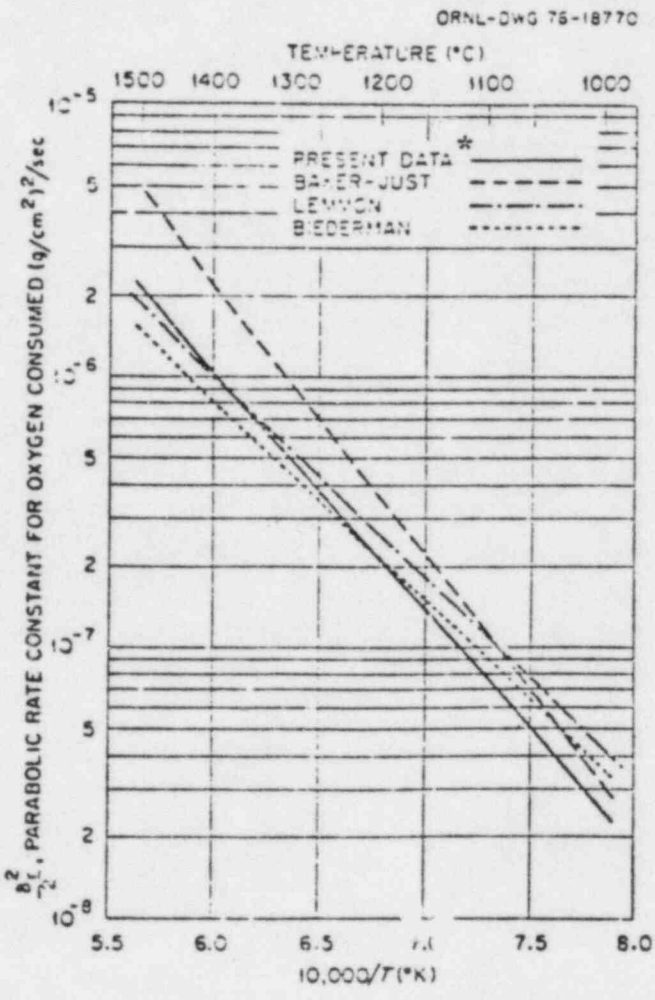

Fig. 3.2. Parabolic Rate Constants for Zircaloy-Steam Reaction [6].
*Cathcart-Pawel Data

Table 3.2 Computed Oxidation Reactions (W)

		Baker-Just	Cathcart	Biederman	Urbanic-Heidrick	
	A	33.3E+06	2.94E+06	3.10E+05	8.79E+05	2.96E+05
	-B	45500	39940	33370	33000	33420
Temp °C	°K					
800	1073.15	0.1342	0.1469	0.2226	0.4087	0.2149
900	1173.15	0.3332	0.3263	0.4336	0.7905	0.4192
1000	1273.15	0.7172	0.6395	0.7608	1.3783	0.7361
1100	1373.15	1.3805	1.1363	1.2299	2.2164	1.1909
1200	1473.15	2.4314	1.8675	1.8628	3.3414	1.8048
1300	1573.15	3.9849	2.8815	2.6762	4.7813	2.5943
1400	1673.15	6.1565	4.2212	3.6819	6.5548	3.5709
1500	1773.15	9.0560	5.9233	4.8865	8.6719	4.7411
1580	1853.15	11.9673	7.5654	5.9949	10.6150	5.8184
1600	1873.15	12.7834	8.0164	6.2921	11.1352	6.1072
1700	1973.15	17.4253	10.5214	7.8971	13.9403	7.6676
1800	2073.15	23.0535	13.4517	9.6965	17.0779	9.4177
1900	2173.15	29.7239	16.8136	11.6832	20.5344	11.3504
2000	2273.15	37.4769	20.6072	13.8479	24.2933	13.4569
2100	2373.15	46.3382	24.8273	16.1803	28.3360	15.7271
2200	2473.15	56.3197	29.4644	18.6690	32.6426	18.1500
2300	2573.15	67.4212	34.5053	21.3023	37.1925	20.7142
2400	2673.15	79.6319	39.9340	24.0683	41.9648	23.4081

☐ Out of range

than those predicted by their analytical expression derived from the data for oxidation in pure steam, although the authors attributed this difference to statistical uncertainties. However, the authors were unable to conclude that these impurities had no measurable effect.

3.1.3 Urbanic - Heidrick.

Another detailed series were carried out by Urbanic and his associates at the Chalk River Laboratories in Canada [8,9]. These studies measured reaction kinetics and the rate for growth of the combined (ZrO_2 + alpha-Zr) layer for zircaloy-2 and zircaloy-4 oxidation in steam over the temperature range of 1050-1850 C. The method involved induction heating of cylindrical zircaloy-2 and zircaloy-4 samples in flowing steam. The weight gain and hydrogen evolution were measured. Measurement of weight gain permitted investigation of the possibiity of the reaction being limited by hydrogen blanketing (gas phase diffusion limited reaction). The results showed 1) the reaction rates given by the Baker-Just correlation are higher than those measured by Urbanic et al. below 1580 C, and above about 1580 C the data more closely follows the Baker-Just correlation, 2) the zircaloy/steam reaction rate was not limited by gas phase diffusion, 3) that there was a sharp transition in the reaction rate corresponding to the cubic-tetragonal phase transition in the oxide at 1580 C. Thus Urbanic et al. found their data to be best fit by the use of two separate sets of rate constants, one set describing the region below 1580 C and the other set above.

The rate of reaction was found to be independent of the gas flow rate. Also the average rate constant is the same as that obtained with 100 % steam flow. Thus, the reaction was not gas phase diffusion limited.

3.1.4 Biederman - Ocken.

Another comprehensive study of the oxidation kinetics was carried out by Biederman and his associates at the Worcester Polytechnic Institute (WPI) [10-12] and by Ocken of EPRI [13,14]. The experiments were performed on PWR reactor grade beginning of life zircaloy-4 tubing under controlled

and unlimited steam flow conditions at low temperatures. The tubes were heated by electrical resistance to maintain an electronically controlled temperature.

Results showed that oxidation on the outside of the cladding is slightly greater than that on the inside. A comparison of oxidation rate with Klepfer's [15] and the Baker-Just correlations has shown that there is an excellent agreement with Klepfer's in the 982 - 1482 C range, and the reaction rate was 45 % less than the Baker-Just equation at 1482 C and the deviation became greater above that point with increasing temperature. In addition, oxidation of zircaloy-4 was found to be independent of steam superheat temperature and steam flow. Only steam starvation and/or trapped hydrogen appeared to lower the rate of oxidation in steam.

Ocken went further to show that the high temperature Zr-steam oxidation data fell into two groups according to the methods used to heat the specimens during the experiments [13], see Fig 3.4. (Taking this into account, one discovers that the data obtained by a certain heating method are in much better agreement with each other.) Fig 3.5 shows that, at low temperature, the correlation based on the data where the specimens were internally heated is more conservative in that a predicted reaction rate could be as much as 10 % more than that computed by the correlation based on the data from the externally heated specimens. At the high temperature, the converse is true. Therefore, given a choice, it is more conservative (even more than Baker-Just) to use the internal heating approach (e.g., Biederman and Urbanic-Heidrick) at low temperatures (below 1000 C). At the mid temeprature range (1200-1300 C) they are about equal and at the high temeprature range, the external heating method (e.g., Cathcart up to 1500 C) is more conservative.

3.1.5 Others.

Four other correlations often cited in the literature are: Aly and Leistikow (both of KfK), Westerman (PNL), and Suzuki (JAERI). The rate constants determined by their studies are shown in Table 3.1.

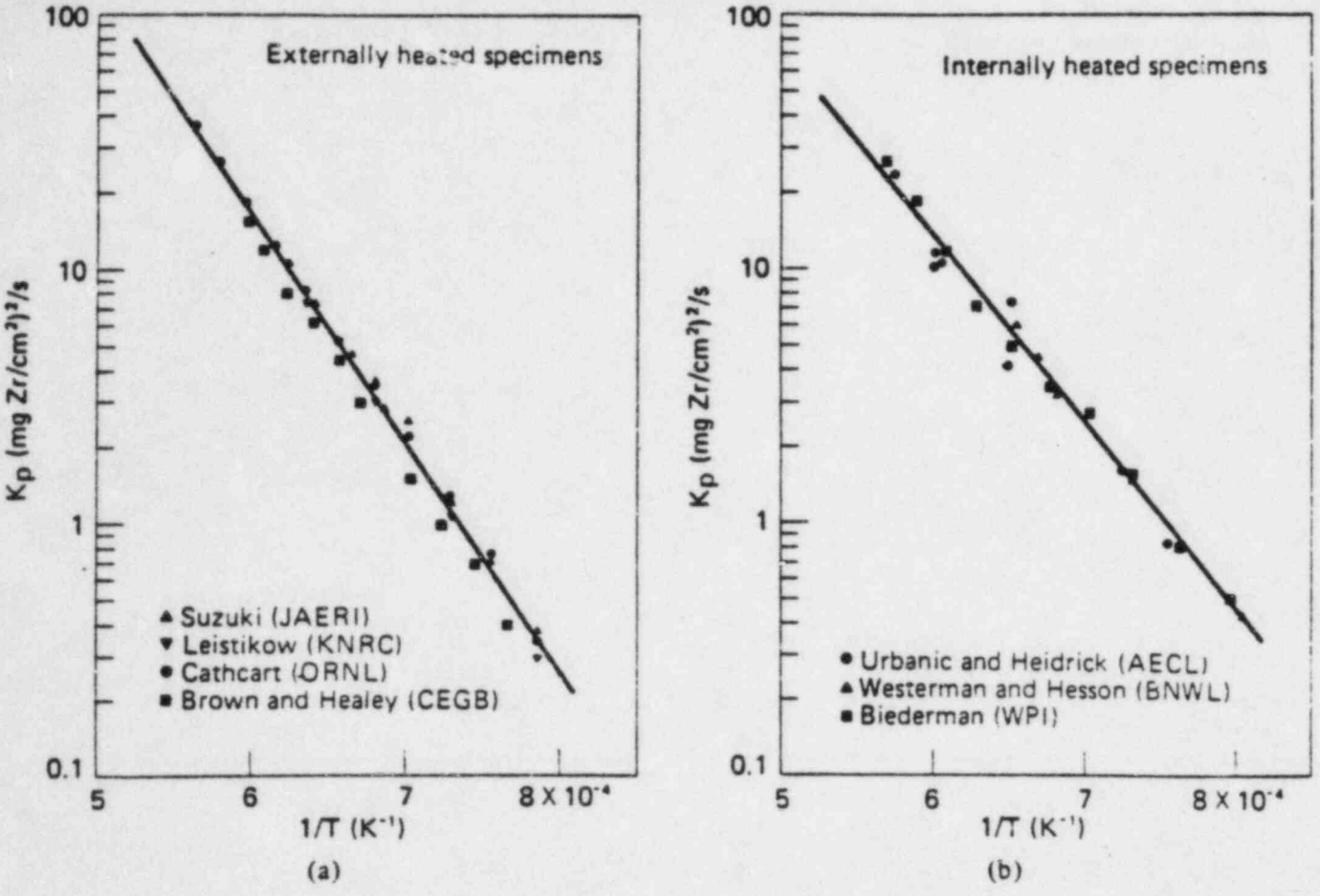

Fig. 3.3. Best-estimate Fit to Parabolic Rate Constant Data for Reacted Zirconium: (a) Externally-heated Specimens, and (b) Internally-heated Specimens [14].

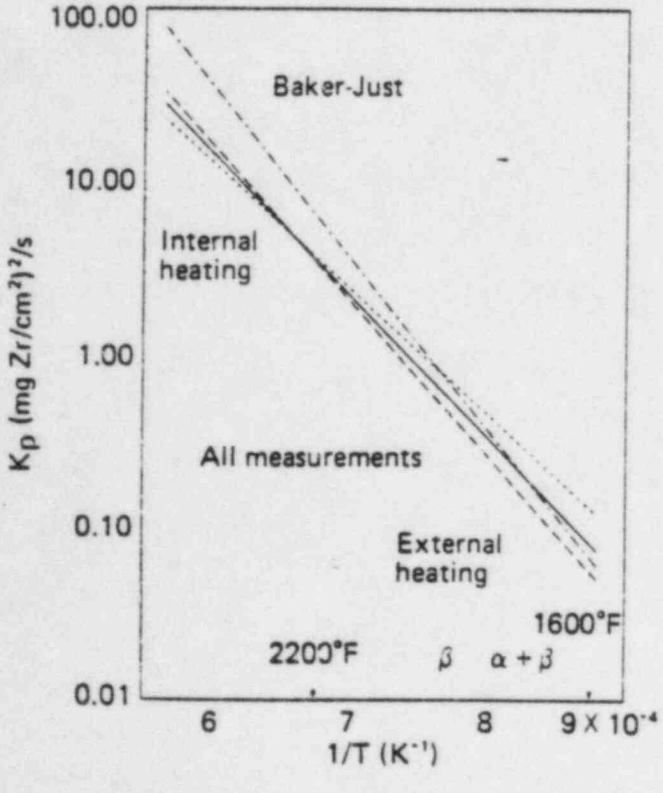

Fig. 3.4. Oxidation Rate of Zircaloy according to Specimen Heating Method [14].

As did Urbanic and Heidrick, Aly measured reaction kinetics [16] over the temperature range 1300 - 1600 C and found a discontinuity in the temperature dependence of the reaction rates (an increase) at 1550 C which he attributed to the change in the oxide microstructure at that temperature. Confirming the effect observed by S. Hagen, Aly also reported that the pre-oxidized tubings oxidized slower than the as-received specimens.

Another study at KfK by Leistikow, et al. [17,18] produced results between 700 and 1300 C which agreed quite well with all others discussed in this report in this range.

Westerman, et al. [19] of PNL generated high temperature zircaloy oxidation data to augment existing data in the range 1255 - 1644 K during the time he performed experiments to determine the relative amount of inside and outside cladding surface oxidation on simulated UO_2-filled, Zr-4 fuel elements ruptured under conditions approximately those expected during a LOCA. He then expressed the rate constants in terms of H_2 liberation and Zr consumption. His equation predicts lower reaction rate than does the Baker-Just equation (as much as 50 % lower at 1422 C).

Suzuki, et al. at Japan Atomic Energy Research Institute (JAERI) investigated zircaloy steam reaction and embrittlement of the zircaloy tube under postulated loss of coolant accident conditions over the reaction temperature range of 1184 to 1330 C. Their computed reaction rates agree well with those of Cathcart and Pawel in this range.

3.2 Experimental Data Supporting Rate limiting Mechanisms.

In this Section, we discuss in detail two separate effects tests at ANL and PNL in an isothermal environment, and two series of integral tests, performed at KfK and INEL, whose objectives were to investigate and identify the oxidation retarding mechanisms and/or to understand the phenomenology of zircaloy oxidation by extending the test temperature range beyond 2000 C.

3.2.1 ANL Experiments.

Two major experiment series were performed at Argonne National Laboratory led respectively by L. Baker and by H. Chung. Baker performed his experiments in the early 1960's [2] and formulated the well known Baker-Just water-metal reaction rate equation which became the foundation for all ensuing other work. His work was discussed in Section 3.1.1. This section presents work by H. Chung [3,21] who challenged the validity of the generally accepted concept that the reaction is not dependent on the steam-hydrogen ratio except at very high temperatures where gaseous diffusion can become important. He identified, though it still remains very controversial, one form of hydrogen blanketing as one of the oxidation limiting mechanisms.

Experimental Procedures

The test specimen, with welded thermocouples, was placed in the center of a Bell jar facing a pyrometer through a quartz window. The material used in his investigation was zircaloy-4 cladding tubes. The bottom end of the 90-mm long specimens was tightly sealed to prevent the steam or the hydrogen-steam mixture from entering the specimen inner space, however, the top end was left partially open to simulate the fuel cladding rupture that is expected to occur in a degraded-core-accident situation. Consequently, the specimen inner surface was exposed during the transient to a hydrogen-rich environment containing a limited amount of steam.

Experiments were performed in three different ways. One set of experiments was initiated by admitting steam at a prescribed rate to an evacuated Bell jar containing the specimen, which was resistively heated and maintained at a constant temperature by control of the current supply. The other experiments were performed in a similar way except that an initial pressure of either hydrogen or helium of about 33 kPa was present in the Bell jar before the steam flow was initiated. Experiments at low temperature showed a definite but not a large effect on reaction rate caused by the presence of an excess of hydrogen. Two possible kinetic limitations were considered responsible for the effects noted: (1) a

decrease in the level of oxygen on the surface of the oxidizing metal such that the reaction becomes controlled at the surface rather than by diffusion through the oxide-controlling layers, (2) the presence of significant quantities of hydrogen in the growing oxide film. The latter effect was considered to have been responsible for the overall decrease in the parabolic oxidation rates [2]. Nevertheless, neither Chung nor any other investigator has attempted to measure the isolated effect of hydrogen buildup in the ZrO2 lattice upon the lattice's diffusion rate constants. (We note that the temperature dependence of such constants could be separately analyzed, and therefore that experiments at moderate temperatures could satisfactorily identify and quantify this effect.)

Results and Discussion

1) For all the steam supply rates, the oxidation kinetics in a pure steam supply were parabolic and the rate constants were a function of specimen temperature only.

2) Oxidation rates for zircaloy-4 tubes in the range 1216-1705 C were slower in hydrogen-steam mixtures than in pure steam or helium-steam environments, see Fig. 3.5.

3) Oxidation in hydrogen-steam mixtures was found to be parabolic or linear depending on the zircaloy temperature, pressures of steam and hydrogen at the gas/oxide boundary, and oxide layer thickness. The linear oxidation rates are smaller than the parabolic rates and indicate that the overall oxidation rate is controlled by gaseous diffusion of hydrogen and by surface reaction between the gaseous hydrogen in the boundary layer and chemisorbed oxygen species on the oxide surface rather than by diffusion of oxygen through the lattice.

4) The parabolic oxidation rate in a hydrogen-steam mixture decreases with decreasing partial pressure of oxygen at the gas/oxide interface, i.e., increasing hydrogen-to-steam ratio. At temperatures greater than 1500 C, the retardation of the parabolic oxidation rate relative to pure steam for a given gas flow and hydrogen-steam composition was found to be more pronounced at higher temperatures, see Fig. 3.5.

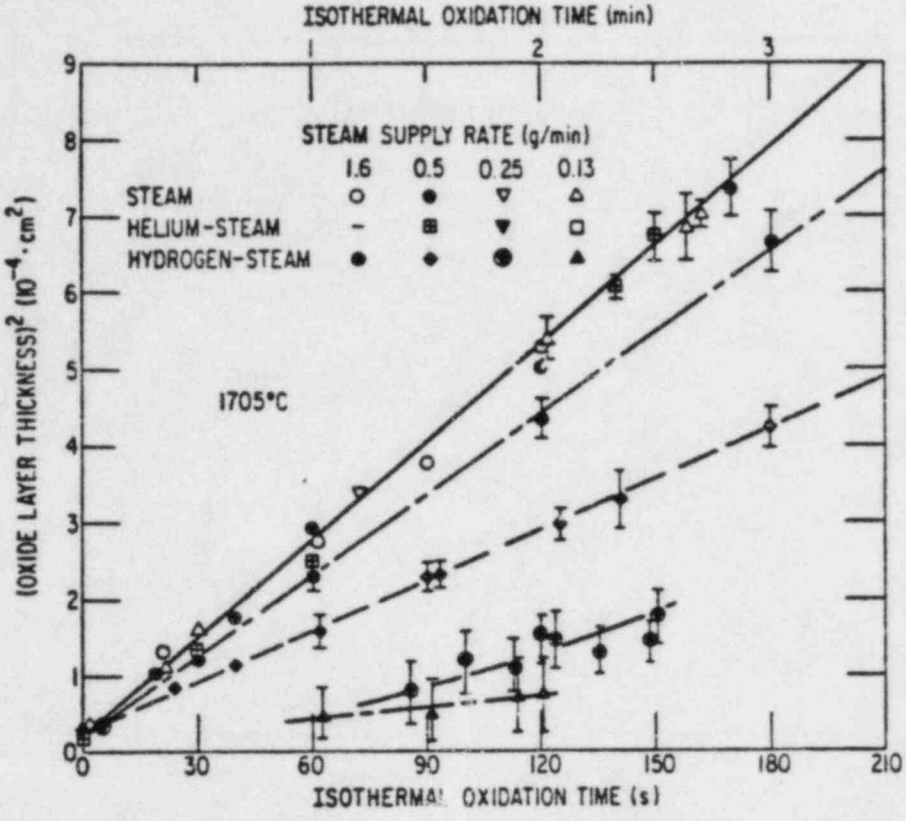

Fig. 3.5. Oxide Layer Thickness vs Time for the Zircaloy-4-Steam Reaction at 1705 C [3].

5) The parabolic oxidation rate reduction in a hydrogen-steam mixture was explained by Chung on the basis of an oxygen transport model of ZrO2-x in which a considerable amount of hydrogen is dissolved in the oxide phase, and as a result, the oxygen vacancy concentration in the oxide near the gas/oxide boundary was increased, thereby reducing the vacancy concentration gradient and therefore the resulting oxygen ion transport rate across the oxide layer.

The critics of Chung's findings argue that in L. Baker's earlier work with the condensor discharge method, the experiments were performed in small volume cells partly filled with liquid water but with no inert gases present initially. As hydrogen was generated by the reaction, it rapidly became the predominant gas phase constituent, the only other one being water vapor. Thus, most of the Baker-Just experiments were performed in a hydrogen-rich atmosphere. Hence, the implication that there is a very large inhibiting effect at high temperatures appears to those critics to be inconsistant in the presence of excess hydrogen [1].

3.2.2 Hagen Experiments.

Out-of-pile experiments were performed to investigate the meltdown phenomena of uranium dioxide/zircaloy-4 fuel rods [22] and to investigate the escalation in temperature of zircaloy-clad fuel rods during heatup in steam due to the exothermal zircaloy steam reaction and processes leading to an escalation retardation in the ESSI (escalation and single fuel rod) and ESBU (escalation in a bundle geometry) series of experiments [23-27].

In the set of meltdown experiments, Hagen found that the long term meltdown behavior (as determined by post-test examination) was influenced mainly by two facts: (a) The chemical interaction between the components of the fuel elements (pellet-can, can-spacer), and (b) the degree of oxidation induced by the metal-steam reactions. The formation of the oxide layer restricted the attack of the spacer to the can, thus meltdown of the can by the spacer was avoided. The post-test examination of the experiments also showed that there was a strong tendency of the melt to stick between the rods [22].

In the following section, the results from the temperature escalation tests, both with a single rod and a nine rod bundle geometries, are presented and discussed.

Single Rod Tests - Experiment Procesures

Several tests were conducted in the NIELS-facility. The fuel rod simulators had lengths of 25 cm and 37 cm. A tungsten heater was inserted in the center of an annular UO_2 pellet (ID of 6.1 mm and OD of 9.2 mm). The zircaloy cladding had the original pressurized water reactor (PWR) dimensions. A zircaloy shroud was placed around the fuel rod simulator to simulate the effect of the surrounding rods, which would also follow the escalating temperature.

Steam was brought into the shroud by a double tube system containing four holes symmetrically arranged assured a uniform supply of steam to the

surface of the rod. Temperature measurement was accomplished by two-color pyrometers.

In order to produce ideal conditions for escalation in ESSI-1 (i.e., an oxide layer as small as possible) the rod and shroud were heated in argon. The voltage was raised stepwise until a temperature of about 1700 C was reached, then the voltage input was held constant. The shroud reached a temperature of about 1200 C by radiation heating from the rod. Once these initial conditions were obtained, a steam flow of 35 g/min was suddenly introduced to start the oxidation.

In all other tests steam was introduced into the vessel from the start, which has an initial argon pressure of 10 kPa. In these other tests, however, the voltage was raised continously in a nearly linear fashion and then held constant.

Single Rod Tests - Results

In the ESSI series, the escalation of the oxidation rate was found to develop faster, and to begin at a lower temperature, if less time was spent in the temperature region below 1200 C. The escalation was greatest (as expected) for the thinnest previously formed oxide layers, as in ESSI-1, and accordingly the steepest temperature rise was for the test ESSI-1 which reached just above 2200 C. However, in less than a minute the temperature dropped rapidly to below the measuring limit of the pyrometer due to strong steam cooling. Only a small amount of the zircaloy was consumed by oxidation at the time the melting temperature of zircaloy was reached. A large amount of the molten zircaloy was observed by post-test examination to have runoff and refrozen at the lower end of the rod and shroud. Therefore, runoff of the molten zircaloy from the reaction zone was one potential limiting mechanism in the ESSI-1 test [24]. However, since the timescale for runoff was not measured and has not been uniquely analyzed, it cannot be said with any certainty that such runoff was the cause of the very rapid cutoff of oxidation, which seems instead to have been caused simply by cooling due to heat transfer to the steam or to geometry changes.

In all the Hagen tests an escalation peak was observed. The temperature at which the escalation began increased from ESSI-7 (below 1200 C) to ESSI-4 (around 1600 C). Depending upon the initial temperature rise, caused by the different electric power ramps, different oxide layer thicknesses were formed by the time specific temperatures were reached, thus higher temperatures were necessary to get the same reaction rate for slower initial heatup rates. All of these results are, obviously, expected results of the already known dependence of the rate upon existing oxide layers. The maximum temperature in all tests stayed below 2100 C, and the highest temperature was reached in test ESSI-6. The final maximum heatup rate was nearly the same for all tests (around 6 C/s). Also, the gradient of the temperature decrease was similar for the different tests (around 1.2 C/s) due to the use of the same geometrical arrangement and insulation, hence similar heat losses [24].

Hagen also found that the damage to the fuel rod increased with heatup rate which is directly connected to oxygen uptake. The thickness of the oxide layer produced during the test decreases with the externally imposed heatup rate produced by the tungsten heater. The fast externally generated temperature rise keeps the oxygen concentration in the zircaloy low. Results from the ESSI-7 test showed that in the upper part complete annular pellets were dissolved by the molten zircaloy. The molten alloy was observed to have run down into the lower region and refrozen between rod and shroud.

Bundle Geometry - Experimental Procedures

The bundle was composed of a 3 x 3 array of fuel rod simulators surrounded by a zircaloy shroud which was insulated with a 6-mm ZrO_2 fiber ceramic wrap. The fuel rod simulators used here are similar to those used in the ESSI tests with a heated length of 400-mm. A steamflow of 0.093 g/s per rod was inlet to the bundle. Power was applied sufficient enough to cause about a 2 C/sec heating rate until the temperature escalation due to zircaloy oxidation heating raised the heatup rate to about 6 C/sec at which point the external power was cut off.

Temperatures were measure by two color pyrometers on three surfaces: a) shroud outer surface, b) cladding surface of a side rod, and c) clading surface of the center rod.

Bundle Geometry - Test Results

Because the center rod had the smallest net radial heat losses, due to radiative contributions from the surrounding rods and higher local steam temperature, the temperature escalated first at the central pin and reached a maximum of about 2250 C (2523 K - which is roughly 400 degrees above the melt transition of zircaloy). A rapid temperature turnaround was observed at the peak, which has been speculated by the experimenters to have been due to molten zircaloy runoff from the reaction zone. (No direct transient data were obtained which support this speculation, and such a cutoff could have been due to a number of other mechanisms. In fact the time measured between reaching melt temperature and the eventual peak was only a matter of several seconds. In such a time it is physically unlikely that substantial relocation of materials could have taken place. Thus the cut-off may very well have been due to another mechanism, such as changes in the surface to volume ratio accompanying the melt transition and perhaps a resultant of local steam starvation). The temperature of the side rods did not rise nearly as rapidly due to the greater heat losses to the surroundings, which reduced the reaction rate and prevented a marked temperature escalation from occurring [26].

The bundle insulation and shroud were intact following the test. However, both had become severely embrittled and broken into small pieces during dismantling. The cladding from all nine rods had melted over the center portion of the bundle, formed a eutectic with some fuel, flowed down the rods, and frozen in a solid mass near the bottom of the bundle that almost completely blocked the coolant flow channels. Near the bottom of the blockage the relocated cladding was significantly oxidized. The cladding at the upper end of the bundle remained intact but was also substantially oxidized.

It is significant to note that the post-test examination showed that the melt had dissolved both fuel and oxidized cladding and had itself been oxidized by steam. The oxidized melt is a homogeneous $(U,Zr)O_2$ mixed oxide, and it has been speculated that it may have refrozen at a relatively high temperature as a result of increased oxgygen content due to oxygen diffusion through the ZrO_2 [26] raising the melting point.

Conclusions

1) The maximum measured surface temperature was well above the zircaloy melt transition and well above the "cutoff" temperature proposed by various analysts about 2200 C (2473 K) for the single fuel rod test and about 2250 C (2523 K) for the bundle test. See Fig. 3.6.

2) The results of the single rod experiments showed that, independent of the initial heatup rate, a temperature escalation was observed in every test, however the temperature at which the escalation began increased with decreasing initial heatup rate due to reaching autocatalytic conditions with a different build up of ZrO_2 layer thickness. For fast initial heatup, runoff of molten zircaloy was claimed to have been a limiting process for the escalation. However, it is unlikely that ssubstantial run off could have physically taken place in such a time frame, and the cut-off is probably due to some other mechanism, although run off would ultimately take place.

The end result damage to the fuel rods increased with the externally imposed initial heatup rate because the cladding was less oxidized at the time the reaction rate escalated. For slow heatup rates almost no interaction between the oxidized cladding and the UO_2 was observed. For fast heatup rates the entire annular pellet was observed by post-test examination to have been dissolved by the molten zircaloy.

3) For the 9-rod bundle test, the runoff of the melt was again claimed to have limited the escalation of the temperature because post test examination found that cladding from every rod had melted, liquefied some fuel, flowed down the rod and frozen in a solid mass that substantially

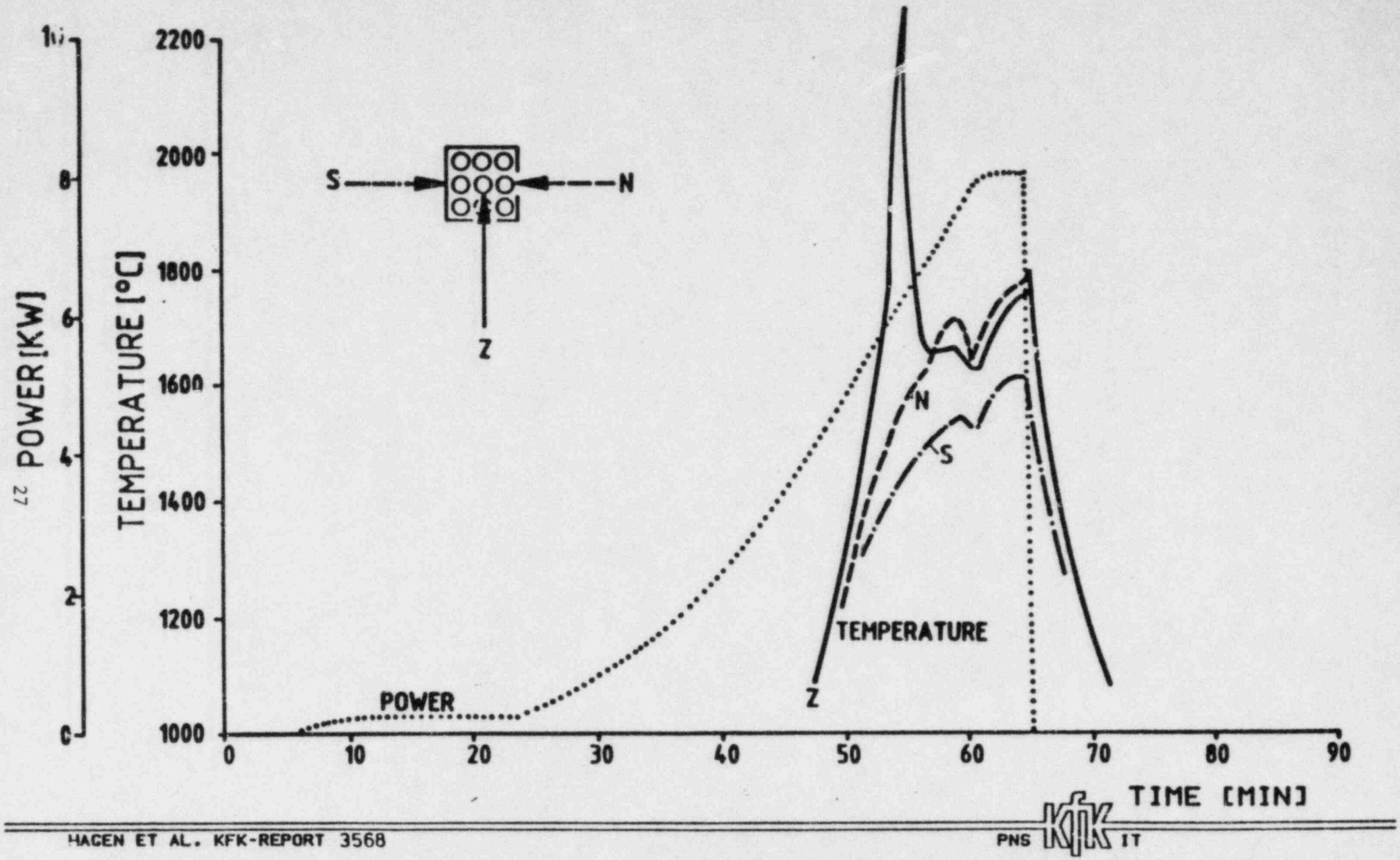

Fig. 3.6. Temperatures on the Central Rod (Z), Side Rod (N) and Shroud (S) 145 mm from the Upper End of Cladding Compared to the Electric Power Input for ESBU-1. [27]

blocked all flow channels. Nevertheless, little analysis has been done which supports such an hypothesis.

4) Post-test examination showed that the melt itself had been oxidized by steam.

3.2.3 PNL Experiments.

The stated purposes of this experiment performed by J. Prater and C. Courtright at Pacific Northwest Laboratory (PNL) [28] were twofold: (1) to extend the oxidation kinetics data on zircaloy-4 in steam to 2400 C, and (2) to study the effect that large quantities of hydrogen may have on the zircaloy oxidation kinetics.

Experimental Procedure

To measure the high temperature oxidation kinetics of zircaloy, an apparatus with low thermal inertia was devised which employed a laser as the source of energy to heat the sample. Oxidation kinetics were established by exposing samples to flowing steam for varying times at nominally the same temperature and then metallographically examining each sample to determine the growth behavior of the oxide layers. Experiments were performed on disk shaped specimens (3.8 mm dia. x 0.9 mm thick) that had been machined from a reactor grade zircaloy-4 bar.

A defocused CO_2 laser beam with a maximum power output of 400 W was used to heat the samples from one side. The surface temperature of the sample was measured using an Ircon two-color pyrometer calibrated regularly against an internal radiation source. Temperature measurements were considered accurate to within 15 C.

The specimens were first heated to a predetermined temperature plateau in argon. Steam, preheated to 600 C, was introduced through a fast-acting valve at a rate of 3 g/m into the test chamber. The ensuing oxidation resulted in a rapid rise to the desired temperature which was then held

constant by controlling the laser heat input. Impliedly, therefore, the oxidation heat generation rates were never as great as the heat losses, since if this were not the case the temperature would continue to rise. Each test was terminated after the desired time increment by closing the shutter on the laser. This resulted in a rapid "quench" of the sample, at an initial rate of 500 C/s.

Because the specimens were heated only from one side, this heating technique produced sharp temperature gradients across the thickness of the sample; the temperature varied linearly with the oxide thickness, each 100 micro-m of oxide thickness reduced the temperature by about 50 C.

A minimum of 5 specimens comprised the data set at each temperature. The small amount of oxidation that occured during the initial exothermic reaction while heating the sample up to its test temperature was measured independently and used to correct for t = 0. In the isothermal oxidation tests, measurements of the oxide and alpha layer thicknesses were obtained at 100 C intervals for temperature between 1300 - 2400 C. In addition, transient tests were performed in steam-hydrogen mixtures varying from 0 to 100 % steam.

Results and Conclusions

1. Parabolic growth kinetics were found to apply over the entire temperature range studied. The linear relationship between the thickening of the reaction layers vs the square root of time confirms that the zircaloy-steam reaction obeys parabolic kinetics, which suggests that the reaction is solid state diffusion controlled, a conclusion reached by virtually all prior oxidation studies conducted above 1200 C. This was further supported by the fact that oxide growth rates were found to be, over the range examined, independent of steam flow rates (from 3 to 19 g/min) and steam pressures (0.1 and 0.5 MPa), indicating that the reaction was not limited by properties of the gas outside the sample.

2. Comparison of the ZrO2 growth rate measured in this study with those of

Cathcart-Pawel, Urbanic-Heidrick, and Baker-Just shows excellent agreement for temperatures below 1500 C between Cathcart-Pawel and the PNL data. Above 1510 C, the kinetic rates increased to rates greater than those of Baker-Just and Urbanic-Heidrick.

3. A discontinuity in the growth rate was observed around 1510 C. This is generally believed to be the result of the change in oxide crystal structure from tetragonal to a duplex tetragonal-cubic layer. No other discontinuity in growth rate was observed, neither upon melting of the underlying metal between 1850-1980 C nor upon transformation of the duplex (tetragonal-cubic) ZrO2 layer to a single-phase cubic oxide at 2285 C.

4. Large temperature gradients across the oxide thickness alter the cubic/tetragonal thickness ratio above 1510 C and, therefore, may also affect the oxidation kinetics.

5. The melting of the zircaloy was characterized by the presence of ZrO2 precipitates in the metal that are believed to have formed when hypereutectic liquid is cooled through 1900 C. The micrographs of samples oxidized above the melting point of the metallic phases revealed only a thin layer of hypereutectic liquid, which suggests that a steep oxygen gradient existed in the metallic phase, even though it was molten. In this context, the rates observed in this study should represent the oxidation behavior of nonturbulent molten zirconium metal, and the continuity of rates through the melting point of the metal further supports the hypothesis that diffusion through the oxide layer represents the rate limiting mechanism in the oxidation process over the entire temperature regime studied. Such a phenomena would, of course, be discontinuous if some hydrodynamic process caused disruption of the oxide layer once the meterial was molten.

Discussion

There are a few areas where the results of this study may be difficult to compare with earlier studies.

1) Because of the presence of large temperature gradients and the unique heating methods, this series of experiments may not have produced truly isothermal results. The heating technique utilized in this study resulted in large temperature gradients (in some cases in the order of 200 C) across the sample thickness due to heating of only one side of the specimen as well as over the same surface due to a highly localized manner of heating by the laser beam. This makes interpretation of the results very complicated and comparison with other experimental results difficult. In addition, we are surprised that PNL was able to control the sample temperature constant for 40 seconds without overshooting, when the exothermic nature of the reaction can easily produce 500 C rise in temperature over a few seconds.

2) The experimental technique was unique, and may need additional refinement. The sample was first heated in "vacuum" to a pre-determined temperature which was lower than the test temperature. Then steam of the same temperature was introduced. The sample temperature rose due to the exothermic reaction, and then the laser beam was turned on to raise and maintain the sample temperature to and at the test temperature. In spite of the claim by PNL experimenters that, once normalized, the experimental data are independent of past history, there appear to be large uncertainties in the test data which PNL experimenters have attempted to overcome by time shifting and by renormalization to remove otherwise anomalous data.

3) In the actual situation, the cladding oxidizes from only one side since the inside of the pin is in the hydrogen rich environment.

Nevertheless, one major result of these experiments which must not be overlooked is the experimental determination that oxidation continues after melting and is still limited primarily by the build up of an oxide layer on the molten zircaloy, even though the entire zircaloy specimen is molten, through which steam (or oxygen) must diffuse to reach the active region. Thus the concept that zircaloy oxidation is diffusion limited is valid even above the melt transition.

3.2.4 PBF Experiments.

As part of Severe Fuel Damage (SFD) research program to investigate fuel rod and core response and the release and transport of fission products and hydrogen during degraded core cooling acccidents, a series of experiments [29-32] have been performed in the Power Burst Facility (PBF) at the Idaho National Engineering Laboratory. The objective of the PBF test series is to obtain the data necessary to understand (a) fuel behavior under severely degraded conditions; (b) fission product release, deposition, and transport; and (c) hydrogen generation.

There have been four such experiments already performed whose parametrics are:

Table 3.3. SFD Series 1 Tests Parametrics.

Test	Heating Rate, K/s	Inlet Flow (g/s)**	Test Bundle	Cooling
SFD-ST	0.15	16	Fresh rods	Quench
SFD 1-1	0.44 to 1300 K* 1.3 to 1700 K	0.6	Fresh rods	Slow
SFD 1-3	0.44 to 1300 K* 1.3 to 1700 K	0.6	26 irradiated rods 2 fresh rods 4 guide tubes	Slow, argon
SFD 1-4	0.44 to 1300 K* 1.3 to 1700 K	0.6	26 irradiated rods 2 fresh rods 4 Ag-In-Cd control rods in guide tubes	Slow, argon

* Characterized the TMI-2 heatup rates.
** Inlet flow provided by a positive displacement pump during the SFD 1-3 and 1-4 tests, whereas during the SFD 1-1 and -ST, flow was provided by an injection pump.

The SFD experiments were designed to represent the heatup and damage of the fuel in the upper half of a 3000-MW(t) PWR core when peak cladding temperatures reach 2400 K after the core was uncovered during a hypothesized small break loss-of-coolant accident (SBLOCA) without emergency core coolant injection.

The boundary conditions imposed at the SFD 1-1 test are as follow: An LWR core would be uncovered at between 2 and 3 hours after reactor scram during such an accident. The core at this time would have a steam flow of about 4 Kg/s and the primary system pressure would be about 6.9 MPa. The total core power would be about 1.5 % of full power. When scaled to the SFD 1-1 fuel bundle based on the total length of fuel rods in a commercial reactor core, the steam flow rate would be about 0.6 g/s and the total bundle power would be about 8 kW.

The heatup rate in the SFD 1-1 was chosen to simulate the TMI-2 postulated heatup rate. An objective of the SFD 1-3 test was to observe differences in fuel behavior and fission poduct release between fresh (SFD 1-1) and high burn-up (SFD 1-3) fuel rods by attempting to reproduce the heatup rate that occured during the SFD 1-1 test.

Facility Description

Unlike any other test facility, the PBF can replicate the proper initial heating from within the fuel by the use of neutronics heating. However, since the facility is designed to accomodate a wide spectrum of tests, it is necessarily very complicated. The reactor consists of a uranium oxide driver core and central flux trap contained in an open tank reactor vessel. An independent pressurized water coolant loop provides a wide range of coolant conditions within the flux trap test space. The PBF core is a right-circular annulus, 1.3 m in diameter and 0.91 m in length, enclosing the vertical flux trap which is 0.21 m in diameter. An in-pile tube fits in the central flux trap region and contains the test train assembly.

The test train coolant was routed via two flowpaths: (a) the flow from the normal in-pile tube inlet was directed upward into the bottom of the test train assembly, then past the insulated shroud and outlet superheated steam line; and (b) the bundle coolant entered the in-pile tube through separate line and then passed through the bundle.

Fuel Bundle

The fuel bundle arrangements for the SFD-ST and SFD 1-1 test trains are very similar, consisting of 32 zircaloy clad UO_2 fuel rods arranged in a 6 x 6 array without the four corner rods. The fuel rods were of typical 17 x 17 pressurized water-reactor design. The test bundle was contained in an insulating shroud consisting of low density zirconia insulation sandwiched between inner and outer zircaloy walls. In all of the SFD Tests, the target power was 8 kW plus any heat loss through the insulating shroud. The shroud loss was estimated as a function of bundle heatup based on the thermal condustivity of the insulation deduced from the SFD Scoping Test. The reactor power was ramped down at about 40 min into the transient.

The SFD 1-3 assembly used a 32-position array filled with 28 fuel rods and four empty zircaloy tubes representing control rod guide thimbles. In the SFD 1-4 test, these four zircaloy tubes were replaced by four control rods. In both of these tests, twenty-six of the fuel rods were highly irradiated, having attained average burnups from 34.5 to 37.2 GWd/t.

Test trains in all four experiments were highly instrumented to measure cladding inside surface temperatures, fuel centerline temperatures, rod internal pressures, water and steam temperature, shroud temperatures, deposition rod temperatures, plenum wall temperature, relative neutron flux, and coolant flow rates and pressures.

Test Data

SFD 1-1

A power ramp of 0.6 kW/min was initiated at 12 min and the cladding

temperature increased at a rate of 0.44 K/s. The power ramp rate was increased to 1.8 kW/min and later readjusted to 1.2 kW/min and held at this rate until 34 min to compensate for the expected heat loss increase through the shroud. The temperature ramp rate was observed to increase to 1.3 K/s when the cladding temperature exceeded 1300 K. This may be attributed to the onset of the exothermal oxidation of the cladding. When the temperature reached about 1700 K, the temperature ramp rate increased to over 30 K/s and the temperature suddenly rose to an indicated 2400 K at 31 min and shortly thereafter began to turn over even before the power decrease began. Based upon failure of certain thermocouples, the experimenters have postulated that molten cladding liquefied fuel began slumping downward at roughly 38 to 40 min and continued until at least 41 min. However, this speculation is not suppported by any direct transient observation. At least 4 % of the fuel was calculated to have been liquefied in the hottest regions of the bundle.

The heating rate for the SFD 1-1 test was specified to be relatively slow up to about 1600 K and rapid above 1600K, driven by the autocatalytic metal-water reaction. The average heatup rate during the test was 0.44 K/s from 900-1200K, 1.3 K/s from 1200 - 1700 K, and over 30 K/s from 1700 - 2400 K.

Nevertheless hydrogen release measurements indicate that the oxidation of the bundle was steam limited during the two separate peaks in measured release rate (the estimated steam flow rate was 1 cm/s at an inlet flow of 0.6 g/s). A total of 71 g of hydrogen was measured, which corresponds to oxidation of 30 % of the bundle fuel rod cladding and shroud inner liner. The results of the test were "confirmed" by RELAP and SCDAP/MOD0 calculations which were performed after the experiment.

SFD 1-3

Since SFD 1-1, the upper plenum region was completely redesigned, and a different material used in this test as shroud insulation (more efficient insulation). This exacerbated the effort to reproduce the heatup rates experienced during the SFD 1-1. The power ramp rates introduced

during SFD 1-3 were different from the previous rates. The ramp down initiated at 2260 sec. instead of 2400 sec. Inlet flow of 0.6 g/s was provided by a positive displacement pump.

Fuel motion during the SFD 1-3 high temperature transient exhibited three distinct phases:

1. A horizontal motion toward the 90-degree side during the bundle depressurization

2. A slumping motion during the heatup period

3. A rapid relocation of fuel in the lower bundle region during the period of maximum temperature.

Hydrogen release indicates that zircaloy oxidation was limited to 25 % of the active bundle inventory of zircaloy, compared with about 30 % in the Test 1-1. Oxidation termination was assumed to be due to steam starvation. Temperature response during the test was similar to that indicated during the SFD 1-1.

SFD 1-4

Similar to SFD 1-3 in the facility arrangement, the SFD 1-4 test used the control rods in place of open-ended zircaloy guide tubes since a specific objective of this test was to investigate behavior of control rods during high-temperature transient.

The control rod which was highly instrumented ruptured unexpectedly at an indicated temperature of 1175 K, and the other three rods also failed at an estimated temperature of about 1700 K.

Unlike the other previous tests, it was necessary to introduce a small flow of argon through the fuel bundle at the outset of the transient due to pressure instability after the initial boildown and this argon gas sweep

system maintained flow during the high-temperature transient in the same manner. The argon gas, which entered near the bottom of the lower plenum region, passed through the water stored there and carried with it an additional steam flow through the bundle. This extra steam flow resulted in enhanced oxidation and therefore hydrogen generation.

The zircaloy shroud inner liner failed at about 1950 s into the transient indicated by the sudden equalization of pressures in the bundle and in the shroud. The bundle pressure dropped about 0.15 MPa which is about 2.1 % of the nominal bundle pressure. In order to recover from the depressurization in the bundle, the argon gas sweep system flow rate was manually incrased from 1.9 to 4.2 mL/s. Thermocouple behavior and the melt-through detector readings indicate that the integrity of the shroud insulation (zirconia fiber board) and shroud wall were never threatened.

Fuel temperature ramp rates started from about 0.36 K/s (0.5 K/s at the lowest elevation) between about 900 and 1200K, and 0.65 K/s at 1200K to 4.1 K/s at 1700 K. Rapid oxidation began about this time indicated by erratic behavior of the thermocouples indicating a stepwise temperature increase of 50 to 90 K. These behaviors continued until the fuel rod temperature reached about 2300 K at the rate in excess of 17 K/s between about 1940 and 1960 s. (This is about the time the argon gas flow rate was increased). The experimenters believe that the thermocouples began to fail at about 2300 K and, therefore, the maximum temperature indicated by thermocouples of at least 2400 K is not reliable. The damaged thermocouples indicated temperatures reached between 2300 and 2400 K when failed.

The amount of hydrogen generated, although preliminary, during SFD 1-4 was 185 g. This is much higher than that produced during the SFD 1-1 or SFD 1-3 test; 71 and 55 g, respectively. This amount of hydrogen corresponds to oxidation of 68 % of the zircaloy in the fuel bundle and shroud inner liner. The greater oxidation observed in the SFD 1-4 test was believed to have been caused by entrainment of water vapor in the argon sweep gas and/or the generation of steam by hot material entering the lower

plenum water reservoir. (Posttest flow measurments indicate that the original flow area through the bundle is about 98 % blocked). In addition, it is believed that the SFD 1-4 test may have experienced higher temperatures for longer times than any previous test and that the argon gas flow prevented the molten zircaloy from falling and thus subjected it to continued oxidation.

These speculations are based upon a series of SCDAP/MOD1/V0 calculations. (In this version, the temperature threshold for instant dissolution of ZrO_2 by liquefied Zr was 2700 K and no multiplier was applied to solubility of UO_2 in Zr.) When the liquefied cladding was allowed to flow down (candling effect), the computed hydrogen generation was only about 66 g, compared to preliminary measured total hydrogen production of 185 g + 30 g. The calculated total hydrogen production increased to 130 g when the meltdown model was modified in the code so that the fuel rod cladding and the shroud inner liner stayed in place until they attained the melting temperature of ZrO_2. The cladding was extensively oxidized (74 %) in the elevation span of 0.1 to 0.9 m. This extensive oxidation heated the test bundle to a calculated peak temperature of 3000 K. These calculations also predicted a longer time at high temperature for the test fuel.

The SCDAP calculation indicated that a significant amount of fuel rod liquefaction occured. A total of 12 % of the bundle fuel rod and 46 % of the bundle cladding is calculated to have liquified and flowed away.

Discussion

The difference in the amount of oxidation is not surprising if the fuel rods with high burnup were subjected to oxide formation prior to the test. Similarly, in each test there was evidence of some UO liquification by formation of eutectic with Zr. None of these experiments resolves the question of whether the rapid oxidation and the rapid accompanying temperature increase were terminated by steam starvation or by geometry changes in the cladding and/or by the flowing away of liquefied cladding and/or fuel.

In all of these test, the shroud inner liner failed. The zircaloy shroud inner liner is there to simulate the surrounding zircaloy cladding of the other fuel rods in the actual reactor, therefore, it is not surprizing that the liner fails when the melting temperature of the zircaloy is reached at the inner liner. However, the failure of the inner liner does cause a disturbance in the test bundle in that (i) the depresurization is apparent, (ii) the flow pattern can be altered, and (iii) the altered flow pattern may also alter the test geometry by disturbing the flow of molten zircaloy.

There are so many variables to consider in the analysis of the SFD experiment results that the interpretation of the results with respect to any one phenomenon becomes much more difficult than in test of separate effects. Furthermore,SFD 1-3 was plagued with instrument problems, e.g., thermocouple failures, instrument calibration problems, etc., early fuel failure, and substantial uncertainties associated with the computation of the delay times to the gas monitoring system detectors.

By far the results of the SFD 1-4 are most difficult to explain. The amount of hydrogen production was a factor of about 3 higher in this test than the previous tests. The only experimental feature which is different is the argon sweep system which was on throughout the experiment, which might have prevented the molten zircaloy from falling and permitted it to continue to oxidize. However, the SCDAP calculation simulating this scenario predicted about 130 g, about 33 % less than the measured value of 185 g. These measured hydrogen production rate data are currently under investigation.

SCDAP calculations resulted in the bundle temperature reaching almost 3000 K and indicated that the bundle was exposed to a very high temperature for a much longer time that were the previous experiments.

The gamma scan during the post-test examination showed that the original cosine shape of the PBF power profile was distorted and biased downward, probably as a consequence of UO2 dissolution by molten cladding

and a portion of it undergoing the candling effect and penetrated through the lower tie plate.

3.3 Summary of Key Experimental Results.

The following items represent the clear results of experiments:

1. Cladding oxidation rate is governed by a diffusion equation, whose rate constants are functions of the thickness and other physical properties of the oxide layer through which oxygen must diffuse to reach the unreacted zircaloy.

2. Cladding oxidation does not cease at the melting transition, and unless the molten zircaloy is subject to turbulent motion, an oxide film builds up on the liquid which has the same effect as the oxide layer which builds up on the solid.

3. In a bundle geometry, only a small portion of molten cladding forms a eutectic with UO_2. Furthermore, there are no data to support the theoretically based hypothesis that Zr which has formed such a eutectic is no longer oxidizable, but even if it were, such an effect is minimal because only a small fraction of the Zr is involved.

4. There is significant evidence that the buildup of hydrogen in the ZrO_2 alters the diffusion constants; however, no experimentalist has performed any separate effect test to measure the effect.

5. Experimental data support the view that a geometry change takes place at the melting transition, which therefore reduces the oxidation rate.

6. There is definite evidence that zircaloy relocates after it melts. Such relocation will take place at a rate less than free fall due to viscous interactions with the remaining intact fuel and other materials and, to a substantially lesser degree, to the up flow of steam.

7. There is experimental evidence that zircaloy oxidation is not terminated by either melting or relocation, but continues in a diffusion limited mode for the particular geometry it assumes.

8. How to scale these experimental results to a particular plant whether it is a PWR or BWR remains to be a problem. For example, out-of-pile tests at KfK were not pressurized therefore, the ballooning of the fuel pins was not observed, whereas ballooning will almost always be expected in the real situations. PBF SFD test heatup rate was specifically designed to simulate that which was observed postfacto during the TMI-2 accident.

4.0 MODELS IN COMPUTER CODES.

We have examined the models utilized in three codes, MARCH [33] and SCDAP (NRC codes) [34] and the BWR-Core Heatup (an IDCOR code) [35]. The MARCH and BWR Core Heatup codes describe the response of water-cooled reactor systems to severe accidents which lead to core meltdown, whereas SCDAP computes the thermal, mechanical and chemical behavior of a light water reactor fuel bundle, rather than the system, during severe accident transients. All of these codes model zircaloy oxidation, hence the hydrogen generation, similarly with minor differences.

In this section, we review in depth the methods by which these codes simulate zircaloy oxidation and hydrogen generation as well as oxidation limiting mechanisms.

4.1 MARCH 2.

MARCH 2 is an improved version of the earlier MARCH 1.1 code. The development of MARCH 2 was coordinated by Battelle-Columbus with contributions being made by national laboratories and other organizations.

For the sake of computational speed, MARCH lumps fuel, the gap, and the cladding into one material. Thus, the code does not really compute the fuel temperature or the clad temperature, but rather the average temperature of the fuel rod. Although the code contains an input parameter for fuel melt temperature (TMELT) it is only used by the code for bookkeeping of the fraction of corium which has melted. (4130 F is a weighted value recommended by SNL for use in MARCH [36]. (See Table 4.1) Lumping of core materials into a single "corium" material impacts the computed rate of temperature rise of both fuel and cladding materials. During rapid autocatalytic portion of a transient, this lumping causes cladding to be computed to heat more slowly than in a seperated materials model. However, the impact on slow transients (which take minutes or

longer) is minimal. This inability to track separate temperatures for fuel and clad causes the code to be unable to follow clad melting (the clad and fuel melt simultaneously at the corium melt temperature), and therefore to obtain any indication of the local tendency for relocation. Furthermore, MARCH uses only one single axial channel to represent the core, so it is incapable of identifying the onset of melting (in a hot channel) or of computing radial incoherencies.

Table 4.1 Melting Temperatures Commonly Used by MARCH and BWR-CORE-HEATUP [36]

Material	MARCH	BWR
Fuel (UO2)	4130 F	5161 F
Cladding (Zr)	4130 F	3451 F
Channel BOx (Zr)	3365 F	3451 F

The MARCH subroutine BOIL calculates metal-water reaction in the uncovered portion of the core. A mixture level is tracked throughout the transient, and the metal-water reaction below the mixture level is not modeled, except for those core nodes currently slumping into the bottom head. Thus, recovering an overheated or molten core region in BOIL will turn off the metal-water reaction below the mixture level. Only zircaloy cladding reaction is calculated unless the BWR channel box and control blade model is selected. If the BWR model is not used, the masses of boxes and blades may be added to the core heat capacity and cladding thickness to simulate their effects. This optional approach produces distortions in core heating and metal-water reaction.

The reaction rate is given by the minimum of a gaseous diffusion rate or a solid state diffusion rate, thus providing for the potential of rate

limitation by hydrogen blanketing. The solid state limited rate is

$$\dot{X}2 = A/Xo\ e\ (-B/(TR + 460))\ Fh2,\ cm/sec \qquad (4.2.1)$$

where

Xo = thickness of oxidized layer, cm
A, B = reaction constants in Table 4.2
Fh2 = hydrogen blanketing factor

The hydrogen blanketing factors are:

$Fh1 = PS'/P$ and $Fh2 = 1$ for $PS'/P > 0.5$
$Fh1 = (PS'/P)^2$ and $Ff2 = PS'/P$ for $PS'/P < 0.5$

where

PS' = steam partial pressure at the node elevation, psia
P = total pressure, psia.

The hydrogen blanketing factor, Fh1, in the steam deprived region is an approximation to the preliminary data of Chung and Thomas.

The user has an option to replace the gas diffusion rates with the MARCH 1.1 model and the solid-state rate is given by Equation 4.2.1 with Fh2 = 1, and A and B are given by the Cathcart or Baker-Just constants as shown in Table 4.2.

Table 4.2 Solid State Diffusion Constants in MARCH.

	A, cm2/sec	B,R	Range
Urbanic-Heidrick	0.00353	30276	TR < 2876 F
	0.0104	29898	TR > 2876 F
Cathcart	0.0373	36181	
Baker-Just	0.394	41220	

There are four oxidation limiting mechanisms which the code permits the user to either select or define: 1) hydrogen blanketing, 2) oxide layer thickness growth, 3) steam starvation, and 4) use of TMWOFF. Appropriate checks are made during the calculation to prevent non physical values, e.g., steam consumption rate vs the steam supply, the oxide layer growth vs the cladding thickness, the rod temperature vs the input cutoff temperature, TMWOFF, etc.

The hydrogen blanketing factor is multiplied into the both gaseous and solid-state diffusion equations. The reciprocal effect of the oxide thickness on the oxidation rate is also built into the equation. The steam starvation is computed through keeping track of the amount of steam available and comparison to the steam consumption rate. The TMWOFF is provided to enable the user to account for the fact that there are large uncertainties in the phenomena associated with the zircaloy melt and where it may relocate and the reduction in the surface area of zircaloy cladding at which oxidation can take place. The use of TMWOFF turns off cladding-steam reaction after the node temperature reaches TMWOFF.

When the user selects the BWR core model, the zircaloy fuel rod cladding and channel box oxidation is calculated using either the Cathcart or Baker-Just parameters over the entire temperature range, with the hydrogen blanketing factor equal to 1.

As we discussed in Section 3.1.1 the Baker-Just correlation can result in an excessively conservative oxidation rate, producing a reaction rate as much as one order of magnitude higher than the measured rate. In addition, in Section 3.1.3, it was pointed out that the use of the Cathcart constants should be limited to the temperature range of 1050-1500 C as they were derived from the data in that range, have not been verified outside of that range and Cathcart and Pawel explicitly directed readers not to extrapolate these values beyond their valid range. Such an extrapolation would be clearly erroneous because of the step transition in rate constants that occurs at roughly 1580 C. Thus the forced selection of one or the other set of rate constants over the entire range of temperature requires the user to choose an unphysical model. This should be corrected.

$$DZRDT = F \cdot A\ e\ (-B/T)/(2*Thi*\rho_{ox}^2)$$

where

F = hydroggen blanketing factor, set to 1,

Thi = oxide layer thickness of node i,

ρ_{ox} = density of the oxidation product ZrO2,

A and B are given by Table 4.3.

Table 4.3. Zircaloy Reaction Rate Constants in BWR-CORE-HEATUP.

Data	A*	B, K	Range
Biederman	9.32 x 10+5	13760	T < 1102 K
Cathcart-Pawel	2.943 x 10+8	20101	1102 < T < 1850 K
Baker-Just	3.33 x 10+9	22899	1850 < T < TOXOFF+25 K

* (Kg Zr comsumed/m2)2/sec

Although the code has the capability of tracking separate temperatures for fuel and clad, it appears from superficial examination (we do not have access to the code itself) that the code version used prior to June 1985 does not properly account for the heat of fusion of zircaloy. In the original Core Heatup Code [37] (forerunner of both ANCHAR and BWR Core Heatup), this was accomplished by artificially adjusting the specific heat of zircaloy to force the melt transition to take place over a one degree increment at the melting point. This permitted the user to follow the transition and to easily compute the local melt fraction. Based upon personal communication with G.R. Thomas, it appears that the developers of BWR Core Heatup chose not to adapt this technique, and overlooked accounting for the heat of fusion by some other technique. Thus in late June 1985, Mr. Thomas personally modified BWR Core Heatup to utilize the specific heat modification technique.

The BWR code also has an option through input of the temperature, TOXOFF, to cease further computation of oxidation in any node which reaches TOXOFF. Cutoff begins at TOXOFF - 25 K and is completed at TOXOFF + 25 K with the cutoff occurring over an S shaped curve. The developers of BWR Core Heatup felt that since the cutoff is a result of physical restructuring, it is considered to be irreversible, and those nodes reaching TOXOFF do not restart oxidation if they later fall below TOXOFF.

It has been recommended by the code developers that 2400 K be used for TOXOFF (275 K above zircaloy melting temperature), based on upper limit interpretation of results from the Karlsruhe (Hagen) experiments and results from the PBF-SFD 1-1 experiment.

The oxidation retarding mechanisms available to users of the code are: 1) hydrogen blanketing (however, this is currently set to 1. in the code, hence causing no reduction in the oxidation rate due to hydrogen), 2) oxide layer thickness growth, 3) use of TOXOFF, and 4) steam starvation due to blockage or complete comsumption of steamby the lower nodes.

4.2.3 SCDAP.

The Severe Core Damage Analysis Package (SCDAP) was developed by EG&G Idaho at the Idaho National Engineering Laboratory to calculate in detail the thermal, mechanical and chemical behavior of a light water reactor fuel bundle during severe accident transients, but excluding accidents that result in core support structure failure. The code has models for the phenomena taking place in a fuel bundle during a severe accident, as such it has been used extensively in the analysis of severe fuel damage experiments (PBF-SFD).

SCDAP/MOD1 [34] models oxidation of the zircaloy cladding using Cathcart-Pawel (for temperatures less than 1850 K) and Urbanic (for T above 1850 K) parabolic rate equations and computes the zircaloy weight gain, zircaloy alpha layer growth, and ZrO2 layer growth. Oxidation-limiting processes modeled include steam starvation, hydrogen blanketing, zircaloy

consumption, and freezing of external crusts. Oxidation of liquified Zr-U-O mixtures is included, assuming zircaloy kinetics are applicable.

Since the oxidation heat is a significant contributor to the fuel rod heatup during a severe transient, a coupled cladding and UO_2 analysis is performed to solve simultaneosly for cladding and fuel temepratures and oxidation rates. Unlike MARCH, SCDAP models cladding and fuel discretly.

Loss of bundle geometry due to both extensive liquefaction and relocation or quench-induced fragmentation on an individual (representative) bundle component basis is modeled. However, once damage becomes extensive in a given elevation in the bundle, subsequent behavior for that portion of the bundle is modeled using SCDAP debris models based on porous body representations which have not been assessed against experimental results for use in LWR severe accident analysis.

Cladding deformation is based on strain-rate-dependent cladding constitutive equations. The ballooning model uses cladding anisotropic material properties. Because of difficulties in modeling the interaction of ballooning, axial fuel relocation, and fission gas release, the ballooning model is not usually used.

Melting of zircaloy, dissolution of UO_2 by molten zircaloy, breach of an outer ZrO2 layer by the liquefied material, and relocation of liquefied mixtures are modeled. Dissolution of UO_2 by liquefied zircaloy is modeled by Turk's equation, and complete dissolution of ZrO_2 by liquefied zircaloy occurs if the temperature is greater than 2700 K and no dissolution occurs if the temperature is below 2700 K. Motion of Zr-U-O mixture is calculated by considering gravity and friction forces. The changes in material properties as a result of changes in mixture composition due to oxidation and Zr-U interaction are considered. Oxidation of flowing Zr-U-O mixtures and frozen crust is also considered.

4.3 Discussion.

All of these codes compute the basic metal-water reaction in approximately the same way, using similar reaction correlations and at a state-of-the-art understanding of zircaloy oxidation, and therefore use of these correlations and mechanisms to compute the rate of oxidation is acceptable although the particular choice offered MARCH users is not optimum and should be corrected. However, justification for continued use of TMWOFF or TOXOFF in MARCH or BWR Core Heatup is weak, and the models for the phenonema which would act to cut off oxidation are not experimentally verified.

5.0 CONCLUSIONS AND RECOMMENDATIONS

5.1 Conclusions

The experimental foundation for the basic oxide layer diffusion limited rate equation for oxidation is very strong and extends well past the melt transition for zircaloy. Thus, unless unexpected turbulence occurs in the motions of molten zircaloy after relocation begins, the use of the standard formulation which computes an oxidation rate which decreases as the oxide layer (solid or liquid) builds up is well supported. Although experiments were performed in various geometries, the parabolic rate law derived from planar geometry seems to fit the data well, due to at least partially to the wide scatter in data even for an individual experimenter.

There are strong indications that oxidation rate is reduced at some point beyond the melt transition. Hagen and his colleagues have attributed such a reduction to slumping of molten cladding. In addition, Chung has demonstrated the presence of some retarding effect due to hydrogen buildup in the oxide layer during the transient before melting (which was apparantly also observed by Cathcart and Pawel). There are no data to support the hypothesis that zircaloy which forms a eutectic with UO_2 is no longer able to undergo an exothermic oxidation, but, even if there were, the experimental data universally indicate that a small fraction of the zircaloy is involved in such a phenomena. Thus eutectic formation can be ruled out as a major contributor to oxidation rate cutoff.

A major observation of the high temperature experiments is that oxidation continues at temperatures well above the melt transition, and that the oxidation is governed by the same rate equation with roughly the same constants.

The experimental data of Hagen and others do not indicate an abrupt cessation of oxidation. They do, however, indicate a gradual reduction in

the continuing rise of the oxidation rate and eventual cessation. Furthermore, experimental data universally indicate the tendency of molten cladding to slump and form blockages, except in those unphysical tests performed in PBF (SFD 1-4) using a positive displacement pump to force the steam through the bundle at unphysically high pressures. Slumping is therefore clearly one long-term mechanism which impacts oxidation rate in two ways: first, it removes the material from the hot region permitting it to relocate to cooler regions where the oxidation rate is reduced, and; second, it permits the formation of blockages which can impede or eliminate steam flow to higher (hotter) regions.

Nevertheless, the experiments clearly demonstrate that zircaloy which slumps is not immune from further oxidation. There is, therefore, no validity to the utilization of any model which computes an abrupt total cessation of oxidation.

That is not to say, however, that there are not mechanisms which occur as a result of the melting of zircaloy which clearly serve to reduce the oxidation rate and which might ultimately cut off the vast majority of such oxidation (i.e., a total blockage). Thus a model which computes a rapid change in the surface to volume ratio of zircaloy shortly after the zircaloy passes through the melt transition would be physically sound and could, perhaps, even be correlated against some of the experiments. Since the zircaloy is in a maximum surface to volume ratio configuration prior to melting, such a change would clearly retard the oxidation rate. Furthermore, it would appear that experimental data support the belief that such a liquid state continues to oxidize according to the standard rate equation and is therefore subject to the same diffusion limitations (although the theoretical foundation would teach that the rate constants are geometry dependent).

In addition, there is no doubt that slumping will follow melting, and the only question is one of time scale; clearly an assumption that the molten zircaloy simply undergoes free fall is incorrect, since such motions are retarded by viscous drag on the remaining intact materials and, to a

lesser degree, by the upflowing steam (which has a very small effect under expected accident conditions other than reflood, since the flow has little driving pressure head). Thus a model which computes relocation in a conservative fashion would also be well supported by both in-pile and ex-pile experiments.

As a direct consequence of slumping, blockages will undoubtedly be formed and there must be some point at which such blockages could completely block a given BWR bundle. The difficulty in development of such a model is that there are no transient experimental data available which were obtained with real materials (i.e., there is only post-test examination evidence) There are, however, several simultant experiments, such as those of Theofanus, or of Henry, which have demonstrated the capability to quantify the phenomena. Thus a carefully planned simulant could quantify the degree of melting which is necessary to permit the formation of a complete blockage. In the absence of such an experimental foundation, a conservative assumption could be made - i.e., when enough material has melted to form a blockage whose axial extent is 10 times the average pin-to-pin gap, assume total blockage and therefore steam flow cut off.

Similarly, in the absence of direct experimental data defining the absolute change in zircaloy surface to volume ratio which occurs upon melting, a conservative assumption could be made: i.e., upon melting the zircaloy forms droplets whose diameter is the lesser of the diagonal distance among four adjacent pins or the surface tension controlled droplet diameter, (or, if we are so convinced, an assumption that the O_2 saturated zircaloy wets the underlying UO_2 and assumes the corresponding liquid film geometry - note that Hagen's experiments indicate that only a small fraction from eutectic, and therefore only a small fraction wetted the UO_2) and the rate constants are altered by the theoretical difference due to the geometry changes. Such a model would clearly reduce the oxidation rate at that point. A conservative model for slumping could be similarly developed by assuming an unphysically high viscous drag on intact materials.

In sum, while there is no foundation for an absolute cutoff of oxidation short of complete steam starvation caused by a total bundle blockage, the experimental data do support models for a relatively abrupt change in surface to volume ratio of zircaloy following melting, followed by slumping and eventual blockage formation. Finally, we note that experimental data also appear to support the theory that the buildup of hydrogen in the ZrO_2 layer impedes further diffusion of oxygen through that layer, but the degree of such an effect has not been quantified.

5.2 Recommendations

1. Correlation for zircaloy oxidation should be objectively selected by analysts based upon their particular need to perform either a best estimate or a conservative analysis. The Baker-Just correlation is most conservatice (and definitely not best-estimate) at high temperatures (above 1550 C). The Urbanic-Heidrick correlation is probably in the best-estimate in this range. In the intermediate temperature range between 1000 to 1550 C, the Cathcart-Pawel correlation is most widely accepted. Below 1000 C, the Baker-Just correlation is no longer conservative. The Biederman correlation appears to be most conservative in this range, however, the difference between this correlation and the other correlations is not very large, since the magnitude of zircaloy oxidation is very small in this temperature range.

2. MARCH should be modified to preserve conservatism in use of the oxidation rate correlations. No single correlation is adequate over all temperature ranges, therefore the code should be modified to provide the users with the best possible combination of choices (of available correlations). Since this is a simple modification, we recommend that it be done without any delay.

3. The continued use of a fixed temperature dependent cutoff for zircaloy oxidation is not recommended since there is neither physical basis nor experimental support for such a phenomenon.

4. Development of a simple and fast running computer model for the geometry changes which occur upon melting and for the subsequent material relocation is recommended for implementation in MARCH. We view development and implementation as roughly a six person-month task. Such a model would be a realistic approach to the phenomena which HCOG is attempting to crudely model with the temperature cutoff.

5. Although they are second order effects, the remaining gaps in experimental data and analysis are:

   a) Reanalysis of the existing data to consider the geometry properly and to develop appropriate oxide diffusion constants from those data.

   b) Performance of a small series of low to moderate temperature experiments (below significant oxidation temperature) on previously oxidized zircaloy, (or, perhaps, comparison of experiments measuring oxidation rates in pure oxygen and in steam, if any such comparable experimental data sets are available) to measure the effect of hydrogen on the diffusion constants for oxygen through the oxide.

6.0 REFERENCES.

1. L. Baker, Jr., "An Assessment of Existing Data on Zirconium Oxidation under Hypothetical Accident Conditions in Light Water Reactors," ANL/LWR/SAF 83-3, Argonne National Laboratory, 1983.

2. L. Baker, and L. C. Just, "Studies of Metal - Water Reactions at High Temperatures, III. Experimental and Theoretical Studies of the Zirconium-Water Reaction," ANL-6548, May 1962.

3. H. M. Chung and G. R. Thomas, "High-Temperature Oxidation of Zircaloy in Hydrogen-Steam Mixtures," Sixth International Conference on Zirconium in the Nuclear Industry, Vancouver, Canada, September 1982.

4. D. Mason and P. Martin, in Chemical Engineering Division Summary Reports, ANL-6101, February 1960, and ANL-6145, May 1960.

5. R. E. Pawel, et al., "Zirconium Metal-Water Oxidation Kinetics: V. Oxidation of Zircaloy in High Pressure Steam," ORNL/NUREG-31, December 1977.

6. J. V. Cathcart, et al., "Zirconium Metal - Water Oxidation Kinetics IV - Reaction Rate Studies," ORNL/NUREG-17, 1977.

7. R. E. Pawel, J. V. Cathcart, and R. A. McKee, "The Kinetics of Oxidation of Zircaloy-4 in Steam at High Temperatures," Electrochemical Science and Technology, Vol. 126, 7, July 1979.

8. V. F. Urbanic, "Oxidation of Zirconium Alloys in Steam at 1000 to 1850 C," American Society for Testing and Materials, Proc. of the Third International Conference, Quebec City, Canada, August 1976.

9. V. F. Urbanic and T. R. Heidrick, "High-Temperature Oxidation of Zircaloy-2 and Zircaloy-4 in Steam," J. of Nucl. Mat. 75, 1978.

10. R. R. Biederman, et al., "A Study of Zircaloy 4 - Steam Oxidation Reaction Kinetics,' EPRI NP-225, Electric Power Research Institute, September 1975.

11. R. R. Biederman, et al., "A Study of Zircaloy 4 - Steam Oxidation Reaction Kinetics," EPRI NP-734, Electric Power Reseach Institute, April 1978.

12. R. G. Ballinger, et al., "Oxidation Reaction Kinetics of Zircaloy-4 in an Unlimited Steam Environment," J. of Nucl. Mat. 62, 1976.

13. H. Ocken, et al., "Evaluation Models of Zircaloy Oxidation in Light of Recent Experiments," Zirconium in the Nuclear Industry, Proc. of the Fourth International Conference, ASTM STP 681 June 1978.

14. H. Ocken, "An Improved Evaluation Model for Zircaloy Oxidation," Nuclear Technology 47, 1980.

15. H. H. Klepfer, "Specific Zirconium Alloy Design Program," Summary Report GEAP-4504, April 1964.

16. A.E. Aly, "Oxidation of Zircaloy-4 Tubing in Steam at 1350 to 1600 C," KFK-3358, 1982.

17. S. Leistikow, "Kinetics and Morphology of the Isothermal Steam Oxidation of Zircaloy-4 from 700 to 1300 C," KfK-2587, 1978.

18. "Nuclear Safety Project: Second Semi-Annual Report 1977," KfK-2600, 1978.

19. R. E. Westerman, et al., "Zircaloy Cladding ID/OD Oxidation Studies," EPRI-NP-525, 1977.

20. M. Suzuki, et al., "Zircaloy Steam Reaction and Embrittlement of the Oxidized Zircaloy Tube under Postulated Loss of Coolant Accident Conditions (Oxidation Kinetics and Embrittlement of Zircaloy at above 1200 C)," JAERI-M-6879, NUREG-tr-0014, January 1977.

21. H. M. Chung and S. M. Gehl, "Thermochemical Aspects of Fuel-Rod Material Interactions at 1900 C," Proceedings of the International Meeting on Thermal Nuclear Reactor Safety, NUREG/CP-0027, November 1982.

22. S. Hagen and C. Politis, "Jahreskolloquium 1976 des Projekts Nukleare Sicherheit," KfK-2399, 1976.

23. S. Hagen and H. Malauschek, "Bundle Experiments on the Meltdown Behavior of PWR Fuel Rods," Transaction of the American Nuclear Society, Vol. 33, 1979.

24. S. Hagen, "Out-of-Pile Experiments on the High-Temperature Behavior of Zircaloy-4 Clad Fuel Rod," Zirconium in the Nuclear Industry, Sixth International Symposium, ASTM 04-824000-35, 1982.

25. S. Hagen, "Out-of Pile Experiments on the High Temperature Behavior of Zry-4 Clad Fuel Rods," KfK-3567, August 1983.

26. S. Hagen and S. O. Peck, "Out-of-pile Bundle Temperature Escalation Under Severe Fuel Damage Conditions," KfK-3568, August 1983.

27. S. Hagen, et al., "Temperature Escalation in PWR Fuel Rod Simulator Bundles due to the Zircaloy/Steam Reaction Test ESBU-1 Test Results Report," KfK-3508, December 1983.

28. J. T. Prater and E. L. Courtright, "Oxidation of Zircaloy-4 in Steam at 1300 to 2400 C," Seventh International Conference on Zirconium in the Nuclear Industry, June 1985.

29. R. K. McCardell, et al., "Severe Fuel Damage Test Series: Severe Fuel Damage Scoping Test Quick Look Report," EG&G Idaho, December 1982.

30. R. K. McCardell, et al., "Severe Fuel Damage Test 1-1 Quick Look Report," EG&G Idaho, October 1983.

31. R.W. Miller, et al., "Severe Fuel Damage Test 1-3: Quick Look Report," EG&G Idaho, October 1984.

32. R. W. Miller, et al., "Severe Fuel Damage Test 1-4 Quick Look Report," EG&G Idaho, July 1985.

33. "MARCH 2 (Meltdown Accident Response Characteristics) Code Description and User's Manual," NUREG/CR-3988 (BMI-2115), 1984.

34. "User's Manual and Details of Modeling for the BWR Core Heatup Code," SLI-8414, Rev.1, Cambell, CA, 1984.

35. C.M. Allison, et al., "Draft Prelminary Report for Comment: SCDAP/MOD1 Theory and Models," EG & G Idaho, January 1985.

36. J. W. Yang and W. T. Pratt, "Analysis of Hydrogen Production during a BWR6 Core Heatup Transient," Brookhaven National Laboratory, to be published.

37. "A Code for Predicting the Temperature and Oxidation of Undercooled Cores," NSAC-11, EPRI/NSAC, 1981.

Acknowledgements

This report was prepared by International Technical Services, Inc. (Inter-Tech) staff in partial fulfillment of a project under the direction of the Brookhaven National Laboratory, W. Trevor Pratt, Group Leader, Ji Wu Yang, Task Coordinator; for the U.S. NRC Division of Systems Integration, R. Bonero, Director; B. Sheron, Branch Chief for Reactor Systems; J. Rosenthal, Section Leader. W. Lyon of the US NRC RSB also provided technical guidance and review during the preparation of this report, and J. Weeks of BNL assisted in review of the report.

Inter-Tech staff who provided input to this report were H. Komoriya and P. B. Abramson, authors.

Appendix A

Effect of Non-Planar Geometry on the Parabolic Rate Law [2]

The parabolic rate law is usually considered to apply when the reaction rate is controlled by solid-state diffusion. The diffusion of either metal ions or oxide ions through the crystal lattice of the oxide film is usually the slow step. If there are no ageing effects of the oxide film, the rate of increase of oxide film thickness $(x_o - x)$, where x is the inner radius and x_o is the outer radius, will be inversely propotional to the film thickness and expressed in the differential form as follows,

$$\frac{d(x_o - x)}{dt} \quad \alpha \quad \frac{1}{x_o - x} \tag{A1}$$

is rigorously correct only for a solid-state diffusion process occurring at a plane surface. The usual form of the parabolic rate law is obtained by integrating at constant temperature to yield $(x_o - x)^2$. It is also well established that the Arrhenius equation adequately describes the effect of temperature on the reaction rate for many metals. The rate equation can then be expressed in terms of the surface temperature Ts and the activation energy E as follows:

$$\frac{dx}{dt} \quad \alpha \quad \frac{1}{(x_o - x)} \quad \exp\left(\frac{\Delta E}{R\ Ts}\right) \tag{A2}$$

If the pre-exponential factor of the rate equation, A, is expressed in units of milligrams of metal/sq cm, quantity squared per second, the parabolic rate law becomes:

$$-\left(\frac{dx}{dt}\right)_{\text{pababolic}} = \frac{10\text{-}6\ A}{2\rho^2\ (x_o - x)} \quad \exp\left(\frac{\Delta E}{R\ Ts}\right) \tag{A3}$$

Diffusion through a barrier film on a cylindrical or spherical surface must depent not only on the thickness of the barrier, $x_o - x$ but also on the ratio of the inner radius x to the outer radius x_o. This was pointed out by L. F. Epstein and R. E. Carter, both of General Electric in the late 1950's and early 1960's. Epstein derived the correct form of the parabolic rate law for cylndrical and spherical geometry by a detailed solution of Fick's law of diffusion. Carter derived the identical relation for spherical geometry by equating the steady-state equation for diffusion through a spherical shell to the instantaneous reaction rate. Carter's equation also provided for the difference in density between the metal and the oxide.

The equations were derived here by the ANL team by a simple analogy to the flow of electric current. Solid-state diffusion through an insulating crystal can, in fact, be considered as a current of ions migrating under

the influence of an emf. The reaction rate can be identified with the current, and Ohm's law may be formally applied as follows:

$$\text{Reaction rate} \quad \alpha \quad \text{emf/Resistance.} \tag{A4}$$

The electrical resistance is expressed in terms of resistivity for 3 cases as follows:

$$\text{Plane} \qquad \text{Resistance} = \text{Resistivity}\ \frac{x_o - x}{A} \tag{A5a}$$

$$\text{Cylincrical Shell} \qquad \text{Resistance} = \text{Resistivity}\ \frac{\ln[x_o/x]}{2\pi L} \tag{A5b}$$

$$\text{Spherical Shell} \qquad \text{Resistance} = \text{Resistivity}\ \frac{x_o - x}{4\pi x_o x} \tag{A5c}$$

where A is the planar area normal to current flow, and L is the length of the cylinder. The volumetric reaction rate (cc metal/sec) can be expressed as follows for the 3 cases:

$$\text{Plane:} \qquad \text{Reaction rate} = A\frac{d(x_o - x)}{dt} \tag{A6a}$$

$$\text{Cylinder:} \qquad \text{Reaction rate} = 2\pi L x \frac{d(x_o - x)}{dt} \tag{A6b}$$

$$\text{Sphere:} \qquad \text{Reaction rate} = 4\pi x^2 \frac{d(x_o - x)}{dt} \tag{A6c}$$

Substituting Equation A5 into A4 and equating Equation A4 to Equations A6 yield the following:

$$\text{Plane:} \quad \frac{d(x_o - x)}{dt} \quad \alpha \quad \frac{1}{x_o - x} \tag{A7a}$$

$$\text{Cylinder:} \quad \frac{d(x_o - x)}{dt} \quad \alpha \quad \frac{1}{x_o \ln(x_o/x)} \tag{A7b}$$

$$\text{Sphere:} \quad \frac{d(x_o - x)}{dt} \quad \alpha \quad \frac{x_o}{x\,(x_o - x)} \tag{A7c}$$

Equation A7a is identical with Equation B1 and represents the parabolic rate law for a plane surface. Equation A7b and A7c represent the parabolic law for a cylincrical and a spherical surface, respectively.

The error introduced by applying the simplified rate law Euqation A7a to spheres is found by comparing Euqation A7a with Equation A7c.